Lawrence Berkeley National Laboratory

Recent Work

Title

Three-dimensional groundwater flow, aquifer response and treatment system monitoring at Site OU 1, former Fort Ord, California

Permalink

https://escholarship.org/uc/item/55j7r9zd

Authors

Oldenburg, Curt M.
Daley, Paul F.
Freifeld, Barry M.
et al.

Publication Date

2002-01-31

eScholarship.org Powered by the California Digital Library
University of California

LBNL-49586

ERNEST ORLANDO LAWRENCE
BERKELEY NATIONAL LABORATORY

Three-Dimensional Groundwater Flow, Aquifer Response, and Treatment System Monitoring at Site OU 1, Former Fort Ord, California

Curtis M. Oldenburg, Paul F. Daley, Barry M. Freifeld,
Jennifer Hinds, and Preston D. Jordan

Earth Sciences Division

February 2002

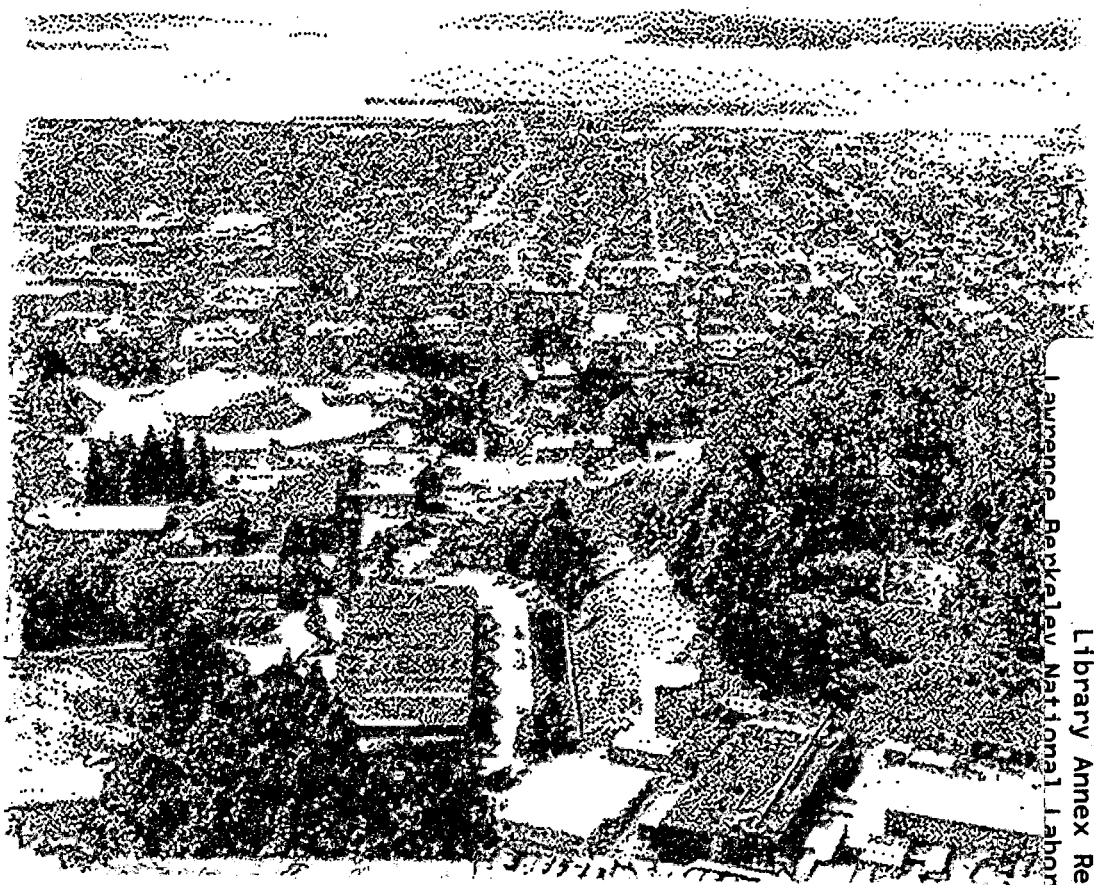

REFERENCE COPY
Does Not
Circulate
Copy 1
Library Annex Reference
Lawrence Berkeley National Laboratory
LBNL-49586

DISCLAIMER

This document was prepared as an account of work sponsored by the United States Government. While this document is believed to contain correct information, neither the United States Government nor any agency thereof, nor The Regents of the University of California, nor any of their employees, makes any warranty, express or implied, or assumes any legal responsibility for the accuracy, completeness, or usefulness of any information, apparatus, product, or process disclosed, or represents that its use would not infringe privately owned rights. Reference herein to any specific commercial product, process, or service by its trade name, trademark, manufacturer, or otherwise, does not necessarily constitute or imply its endorsement, recommendation, or favoring by the United States Government or any agency thereof, or The Regents of the University of California. The views and opinions of authors expressed herein do not necessarily state or reflect those of the United States Government or any agency thereof, or The Regents of the University of California.

Ernest Orlando Lawrence Berkeley National Laboratory
is an equal opportunity employer.

DISCLAIMER

This document was prepared as an account of work sponsored by the United States Government. While this document is believed to contain correct information, neither the United States Government nor any agency thereof, nor the Regents of the University of California, nor any of their employees, makes any warranty, express or implied, or assumes any legal responsibility for the accuracy, completeness, or usefulness of any information, apparatus, product, or process disclosed, or represents that its use would not infringe privately owned rights. Reference herein to any specific commercial product, process, or service by its trade name, trademark, manufacturer, or otherwise, does not necessarily constitute or imply its endorsement, recommendation, or favoring by the United States Government or any agency thereof, or the Regents of the University of California. The views and opinions of authors expressed herein do not necessarily state or reflect those of the United States Government or any agency thereof or the Regents of the University of California.

LBNL-49586

Three-Dimensional Groundwater Flow, Aquifer Response, and Treatment System Monitoring at Site OU 1, Former Fort Ord, California

Curtis M. Oldenburg[1]
Paul F. Daley[2]
Barry M. Freifeld[1]
Jennifer Hinds[1]
Preston D. Jordan[1]

[1]*Earth Sciences Division*
Lawrence Berkeley National Laboratory

[2]*Energy and Environment Directorate*
Lawrence Livermore National Laboratory

February 26, 2002

This work was supported by the U.S. Army Industrial Ecology Center and administered by the University of California, Santa Cruz, through the U.S. Department of Energy under Contract No. DE-AC03-76SF00098 (LBNL) and W-7405-ENG-48 (LLNL).

TABLE OF CONTENTS

LIST OF TABLES

LIST OF FIGURES

ABBREVIATIONS AND ACRONYMS

amsl	above mean sea level.
azi	azimuth
AAF	Army Airfield
ASAP	Analytical Sampling and Analysis Platform
bgs	below ground surface
CAS	Chemical Abstract Service
CalEPA	California Environmental Protection Agency

CERCLA	Comprehensive Environmental Response, Compensation, and Liability Act
CP	Capillary Pressure input variables for TOUGH2
CPVC	Chlorinated PolyVinyl Chloride
DC	Direct Current
dH	Change in head
DTW	Depth To Water
EPA	Environmental Protection Agency
EW	Extraction Well
FDA	Fire Drill Area
FOC	Fraction Organic Carbon
GC	Gas Chromatograph
GCMS	Gas Chromatograph Mass Spectrometer
GIS	Geographic Information System
GPM	Gallons Per Minute (also gpm).
GTS	Groundwater Treatment System
HLA	Harding Lawson Associates (now Harding ESE)
ICFMS	Integrated Chemical and Flow Monitoring System
ISPFS	In Situ Permeable Flow Sensor
MCL	Maximum Contamination Limit
MDL	Method Detection Limit
MW	Monitoring Well
msl	mean sea level
NAD83	North American Datum of 1983
ND	Non-Detect
NOAA	National Oceanic and Atmospheric Administration
OU	Operable Unit
ppb	Part Per Billion
PQL	Practical Quantitation Limit
ROD	Record of Decision
RT	Retention Time
SDM	Surface Data Manager
TOUGH2	Transport Of Unsaturated Groundwater and Heat

UC/NRS	University of California Natural Reserve System
VOA	Volatile Organic Analysis
VOC	Volatile Organic Compound
3D	Three Dimensional

ACKNOWLEDGMENTS

This work was supported by the U.S. Army Industrial Ecology Center through the Concurrent Technologies Corporation Contract No. DAAE30-98-C-1050, Task No. 281, CRDL No. B009 administered by the University of California, Santa Cruz, and by the Ernest Orlando Lawrence Berkeley National Laboratory under U.S. Department of Energy Contract No. DE-AC03-76SF00098, and by the Lawrence Livermore National Laboratory under U.S. Department of Energy Contract No. W-7405-ENG-48.

Numerous people have contributed to this project. First, we thank David Eisen (USACE), Andy Fisher (UCSC), Buck King (Harding ESE) and Larry Friend (Harding ESE) for sharing their wide knowledge of Fort Ord hydrogeology. We further thank Harding ESE (Buck King, Larry Friend, and Ed Heistand) for their generous and efficient work to supply LBNL with monitoring data from OU 1. This report was improved by comments and reviews by Chris Doughty (LBNL), Rohit Salve (LBNL), and Marcelo Lippmann (LBNL). We thank Maria Fink and Diana Swantek (LBNL) for assistance with document conversion and CD preparation. The encouragement and thorough and prompt review comments of Jim Gill (UCSC) improved this report. We further thank Bashar Alhajjar (CTC) for his interest in our work and efficient management of this project.

EXECUTIVE SUMMARY

Introduction

The objective of this project is the development, installation, and testing of state-of-the-art sensor technologies to optimize traditional pump-and-treat remediation of contaminated groundwater. We have installed five in situ permeable flow sensors (ISPFSs) co-located with dedicated low-flow groundwater sampling pumps in the unconfined A-aquifer at a depth of approximately 100 ft (30 m) at the former Fort Ord Army Base, near the Marina Airport. These five wells are thereby instrumented so that both velocity and chemistry can be known at nearly the same location in the same well at the same time.

This new network of instrumentation can be used to investigate key hydrologic questions that have arisen in the course of 12 years of pump-and-treat operations at the site. These questions include: (1) Was the Fire Drill Area (FDA) the only contaminant source of the northwestern plume discovered in 1997? (2) How do clay bodies and (subsurface) flow channels affect the pump-and-treat process? (3) Why are trichloroethylene (TCE) concentrations increasing at certain wells? (4) What is the impact on the groundwater treatment system (GTS) of infiltrating treated water within the capture zone?

A sound understanding of the subsurface hydrogeology and chemistry is critical to testing and interpreting data collected by the new network of instruments, as well as answering the key hydrologic questions. Therefore, in addition to development and installation of the new integrated chemical and flow sensor technology, we have undertaken work in the areas of hydrostratigraphic model development, extensive analysis of existing quarterly monitoring data, active pump testing to perturb the flow field, and three-dimensional numerical simulation.

Geology and Site Description

The investigation area is in the northern part of the former Fort Ord in an area known as Operable Unit 1 (OU 1), located north of Reservation Road near the Marina Airport. The OU 1 area, except for a rectangular 48 acre (0.2 km^2) region surrounding the FDA and groundwater treatment system (GTS), is owned and managed as part of the Fort Ord Natural Reserve by the University of California. The area is covered with highly permeable dune sands and displays hummocky topography.

The subsurface deposits relevant to this study are the result of cyclical periods of sea level rise and fall over the past few hundred thousand years. The marine-to-estuarine clays present in the subsurface at OU 1 and also in the Salinas Valley subsurface represent the uppermost (youngest) deposits of marine transgressions. These clays are collectively referred to as the Salinas Valley Aquitard (SVA),

with the clays at Fort Ord often distinguished by use of a different name, the Fort Ord–Salinas Valley Aquitard (FO–SVA). The timing of deposition of the clays in Salinas Valley and those at Fort Ord is not fully understood, with FO-SVA clays apparently older (>40,000 yrs) than clays in the SVA (<16,000 yrs). Furthermore, the top of the FO–SVA and top of the SVA are at different elevations, the FO–SVA being a few tens of feet above mean sea level, while the SVA is at or just below mean sea level (HLA, 1993). One possible explanation for the relation between the FO-SVA and SVA is that the FO–SVA was deposited during high sea level stands between 100-130 kyr before present while the SVA was deposited during the current modern high sea level stand, which is believed to have been approximately unchanged for the last 10,000 years.

The sedimentary materials in the unconfined A-aquifer consist of fine- to medium-grained, well-sorted older dune sands. The underlying estuarine clays of the FO–SVA for an aquitard beneath the A-aquifer. The thickness of the sands in the A-aquifer ranges from about 90 to 130 ft (27 to 40 m) at OU 1 due to variable topography. The present water table elevation in the A-aquifer at OU 1 is between 40 and 70 ft (12 and 21 m) above mean sea level (with a gradient to the north and northwest), making a saturated thickness of approximately 20 to 35 ft (6 to 11 m) within the study area.

Historically, solvents and fuels were placed in a burn pit in the Fire Drill Area (FDA) and used for fire fighter training from 1962 until 1985 resulting in groundwater contamination consisting of volatile organic compounds (VOCs), primarily trichloroethylene (TCE). Extraction from wells EW-OU1-17-A and EW-OU1-18-A commenced in mid-1988 for the purpose of plume containment and remediation. Water extracted from these wells is passed through an on-site granular, activated charcoal treatment system and then pumped to the south end of the FDA where it is spread over the ground surface by two knocking-head sprinklers. Samples for groundwater contaminant concentrations have been taken quarterly and water level measurements have been taken monthly to quarterly since 1988. New concern for groundwater remediation at OU 1 arose in 1997 when it was confirmed from quarterly sampling that VOCs were in groundwater downgradient from the capture area of the existing GTS. Further investigation through installation of additional wells and monitoring have led to the delineation of a downgradient TCE plume extending 3000 ft (910 m) northwest from the presumptive source in the FDA. OU 1 currently has approximately 70 monitoring wells and two extraction wells in operation.

Installation and Testing of the Chemical Analysis System

In this project, five new wells were installed in 1999. Each well was completed with an ISPFS (HydroTechnics, Inc.) at the base of the A-aquifer, and with a 2 in (5.1 cm) internal diameter monitoring well just above the flow sensor. These wells were outfitted with pressure transducers to measure water depth, and a bladder pump for continuous micropurging of water samples for VOC analysis; five additional existing monitoring wells at the site were also equipped with pressure sensors and pumps. The pump effluent is routed to a central monitoring

instrument facility we installed on the site, where water from each well is automatically selected for VOC concentration analysis. Piping materials for transport of the pump effluent from the wells to the central facility were selected to provide for low loss of target analytes, and to assure that all unions or other junctions were accessible for leak checks. All the pump effluent piping between the wells and the central facility was installed in buried conduit, providing an environmentally friendly installation that could be operated for a protracted period of time with low maintenance requirements.

At the central analytical station water samples are selected for analysis with a custom sample preparation system, and analyzed for VOCs by purge and trap gas chromatography, using methods based on standard EPA protocols and commercially blended analytical standards. Approximately twenty samples are analyzed daily, intermixed with standards that permit semi-continuous assessment of analytical precision. Operation of the integrated system was started in August, 2001; initial data were compared with quarterly monitoring data collected by Harding ESE. Sensitivity of the integrated system was evaluated using the EPA method detection limit approach and by examination of the stability of short term recovery of analytical standards. Method detection limits were within the expected range of conventional analytical laboratories, and detector stability was acceptable over at least a period of weeks. Samples analyzed exhibit plausible trends including short term variations on the order of a few days in some cases. These nearly continuous data are invaluable for understanding contaminant chemistry variability with unprecedented temporal resolution and spatial extent.

Hydrostratigraphic Model Development

The hydrostratigraphic model developed for OU 1 is a simplified, three-dimensional representation of subsurface sedimentary layers believed to control groundwater movement through the unsaturated zone and within the shallow A-aquifer. The hydrostratigraphic model was developed using data describing well locations, lithology (from 70 well logs), and land surface features, such as topography. The resulting model covers an area of 0.34 mi^2 (0.87 km^2). The model is built by stacking layer thicknesses (isochores) of sand and clay on top of the reference horizon taken as mean sea level. The top of the hydrostratigraphic model coincides with the land surface, while the bottom model boundary is mean sea level.

Analysis of the well log data pointed to a multilayered model with eight layers, consisting of four clays separated by four sands. Layer thicknesses vary, and some clay layers pinch out. The shallowest clay is Clay 4, also known as the Airfield Clay. Thickness maps are developed for each model layer based on data contained in the well logs.

Data constraining the clay and sand occurrences at depth are limited, since most wells terminate within the first few feet of the first clay layer encountered. In most cases, wells were logged using cuttings, an approach that prevents the

determination of the exact depth to stratigraphic boundaries due to the mixing of sediments from different vertical locations during drilling. Approximately 10 wells were logged by coring, which provides better depth control when identifying layer contacts and avoids mixing of sediments. Although variable mixtures of sand, silt, and clay exist in the subsurface at OU 1, the predominant sediments are sand and clay.

Water Level and Contaminant Data Analysis

We used the GIS\Key database system with AutoCAD to aid in our analysis of the 12 years of monitoring data provided by Harding ESE. This system allows data to be queried and displayed on reports, graphs, and maps. Water levels in most of the wells at OU 1 respond to seasonal precipitation. Analysis of precipitation data downloaded from the NOAA website suggests that the average precipitation over the last 10 years at OU 1 is 17.1 in/yr. In 1998, OU 1 had more than twice the average annual precipitation, the effects of which can be clearly seen in the monitoring data. Most of the A-aquifer water levels are still rising from the large rainfalls in 1998 as of the end of 2000. Following the 1998 rainfall events, the cones of depression around the extraction wells decreased, leading to smaller capture zones.

The piezometric surface (water table) for the unconfined A-aquifer contoured from the OU 1 water-level data shows a generalized northwest gradient, with cones of depression around the two extraction wells and a groundwater mound beneath the recharge area. The largest hydraulic gradients are near the edge of the Airfield Clay adjacent to the extraction well EW-OU1-17-A. Piezometric head beneath the Airfield Clay is approximately the same as the head at EW-OU1-17-A, implying that flow could move under the Airfield Clay as well as toward the extraction well.

Combining the observed average gradient with an estimate of hydraulic conductivity and porosity in the vicinity of the FDA suggests an average pore velocity of 0.20 ft/day (7.2×10^{-7} m/s). For well spacings on the order of 100 ft (30 m), interwell conservative tracer tests would take on the order of 450 days.

A large downward gradient exists between the A-aquifer and the 180-foot aquifer. The piezometric head in sands confined by clay layers in the FO-SVA screened in well MW-OU1-11-SVA are intermediate between those in wells screened in the A-aquifer and the 180-foot aquifer. The gradient in the 180-foot aquifer is toward the southeast, possibly controlled by agricultural pumping. The water levels in MW-OU1-11-SVA and the 180-foot aquifer wells generally fluctuate more seasonally than water levels in the A-aquifer, probably primarily due to seasonal agricultural pumping. However, the magnitude, duration, and timing of water level changes in these wells after the precipitation in early 1988 suggests at least a portion of the annual variation is due to seasonal recharge. For sand layers in the FO-SVA, this recharge may occur laterally from the Salinas River.

A significant portion of the contaminant migration took place before the onset of pump and treat and associated recharge. However, as water level data prior to this

time were unavailable, we constructed a hypothetical water table without pump-and-treat effects using water levels from wells apparently unperturbed by pumping and recharge. This "perimeter-well" water table uses year 2000 water levels primarily from wells located on the perimeter of the study area. We also constructed an actual 2000 water table using all of the A-aquifer wells. Estimated sprinkler and evaportranspiration losses at the recharge area correlate well with the volume difference between the perimeter-well and actual 2000 water tables. This suggests the perimeter-well water table is a reasonable estimate of the pre-pump-and-treat water table.

The perimeter-well water table gradient points north from the FDA in contrast to the actual 2000 water table gradient which points northwestward. Combining the observed average gradients from the FDA to the northern end of the TCE plume yields an average pore velocity of 0.12 ft/day (0.036 m/day). Multiplying this average velocity by 39 years (the time since start of fire fighter training at the FDA) gives a length of 1680 ft (510 m), which matches the actual plume length to within a factor of two. These results suggest that no additional contaminant sources, hydrogeological heterogeneities, or anisotropies are required to explain the overall TCE plume geometry.

Examination of water level changes at and surrounding EW-OU1-18-A shows that MW-OU1-07-A and MW-OU1-12-A are not hydraulically connected, a fact also observed during pump testing. Similarly, EW-OU1-17-A appears not to communicate with the saturated zone above and below the Airfield Clay, implying that the Airfield Clay is a barrier to effective pump and treat.

The average artificial recharge rate with both extraction pumps operating is about 0.8 in/day (2.0 cm/day) over a 100 ft (30 m) radius area, less 30% for sprinkler and evapotranspiration losses. As water levels increase in the extraction wells, they decline in the recharge area on a 45–60 day time scale. This is due to decreased recharge when the extraction well pumps are turned off. The rapid response of the water table below the recharge area suggests that there are no significant low-permeability layers in the unsaturated zone capable of diverting or attenuating infiltration pulses.

Comparing rainfall amounts to seasonal water fluctuations suggests that approximately 27% of precipitation ends up as recharge at the A-aquifer. Examination of the timing of water level increases associated with the early 1998 precipitation events indicates the infiltration pulse travels through the top 60 ft (18 m) of the unsaturated zone in less than one month. Below this depth, the pulse travels at 20 ft/mo (6.1 m/mo).

Groundwater at OU 1 is contaminated with VOCs, primarily TCE. Increases in TCE concentration at wells to the west of the FDA are probably due to recharge water encountering residual contamination in the unsaturated zone and transporting it downward to the water table. The increases are primarily due to recharge of treated water mobilizing residual contamination, however, the large natural recharge event in 1998 may have mobilized this residual contamination as well. The timing of the TCE concentration increases above the Airfield Clay

relative to the early 1998 precipitation events indicates there may be an additional local TCE source approximately 200 ft (61 m) northeast of the FDA. However, because the northwest plume is generally down-gradient from the FDA, the presence of a significant additional source seems unlikely. Examination of concentrations of TCE degradation products suggests that reductive dechlorination is not an important process in limiting plume length at OU 1.

ISPFS Testing

Short-duration pump tests in the A-aquifer at OU 1 were used to determine that hydraulic conductivity varied from 3.6 ft/day (1.1×10^{-5} m/s) to 42 ft/day (1.5×10^{-4} m/s), with hydraulic conductivity higher in the northwest part of OU 1. We exploited the shutdown of EW-OU1-18-A as a major perturbation to the flow field that could be monitored using the ISPFSs and by measuring depth to water in surrounding wells. Water levels in the recharge area decreased after shutdown in response to less sprinkler recharge. Water levels in wells withing 200 ft (61 m) around the extraction well increased. Wells located farther west, east and north experienced no significant water level changes.

The ISPFSs showed a fast and dramatic response to the extraction well shutdown. Groundwater horizontal velocity and azimuths in three of the five ISPFSs showed plausible changes. One ISPFS is not heating properly, and another produces anomalous flow directions that we suspect may be due to installation error. The ISPFSs show large downward groundwater velocities that are likely an artifact of the nonhomogeneous thermal conductivity field around the instrument. The results from the ISPFSs agree with calculations from a simple model. In summary, the ISPFS appears to be an effective tool to observe changes in groundwater flow in real time.

Flow and Transport Modeling

A numerical grid consisting of 31,888 gridblocks was constructed from the hydrostratigraphic model. This numerical grid was used to simulate groundwater flow and TCE transport at OU 1. We find that the 2000 piezometric surface can be matched fairly well using boundary conditions of constant head as constrained by water level data. The flow directions and velocity magnitudes are consistent with results from water level data analysis and ISPFSs, all of which suggest that long-term monitoring will be necessary for interwell tracer tests.

We investigated the hypothetical flow field that would result from turning off the sprinkler that recharges the A-aquifer. The simulations show that the capture zone is significantly larger for the case of no recharge. Thus the recharging of treated water in the capture zone causes a short-circuit of the GTS and reduces the size of the capture zone. We also simulated the flow field for the current conditions of EW-OU1-18-A turned off, a situation that also results in a smaller capture zone.

Using the perimeter-well water table as the condition prior to 1988, we simulated TCE transport from the presumed source area in the FDA down gradient to the

north for 20 years. With this concentration field as the initial condition along with the flow field of the 2000 water table, we then simulated 12 years of additional TCE transport. We observed in this simulation a northward and then northwestward direction for the TCE plume, as is observed at OU 1. This simulation suggests that the current TCE plume configuration is a natural result of a time-varying water table gradient, and requires no additional sources, anisotropy, or buried flow channels for its formation.

RECOMMENDATIONS

Applications of ICFMS

Test and evaluate the long-term application of the new sensor technologies to the operational scale remediation activities of the GTS. Operation of these new technologies on a sustained basis will help to assess the effectiveness and cost efficiencies of the new sensors.

Take advantage of the rapid response of the ICFMS for chemistry, velocity, and pressure to constrain better the location of potential unsaturated zone remnant VOC contamination sources during infiltration events.

Operate the automated sampling system through the winter and spring months to capture data from natural recharge events that may constrain unsaturated zone flow and transport processes

Correlate short term ISPFS velocity variations with short term oscillations in analyte concentrations. Research in this area may reveal new details about groundwater plume dynamics.

Monitoring and Site Remediation

Continue quarterly monitoring of contaminants and water levels, as this data set has been invaluable in our research and for understanding key features of the A-aquifer at OU 1.

Perform soil gas monitoring with multilevel vadose zone monitoring wells in the unsaturated zone at depth to monitor soil gas concentration changes in response to natural and artificial recharge changes to help locate potential remnant contamination.

Consider disposing of treated water in a different way than recharging in the capture zone. Possible options include misting the water so it evaporates into the air, or discharging it downgradient from the GTS.

Consider alternate locations of disposing of treated water. Additional deployments of ISPFSs could be done to monitor flow directions quickly and accurately such that targeted vadose zone regions could be intentially flushed with subsequent guidance of the resulting recharge toward the extraction wells through selected recharge locations.

Increase the pumping rate from EW-OU1-17-A. This could have several benefits for remediation investigations at OU 1: (1) It would increase the size of the capture zone which seems to have shrunk after 1998; (2) It could serve as a pump test, the response to which could be used to understand the well's effectiveness at controlling downgradient migration of contaminated water from above the Airfield Clay; and (3) the increase in recharge rate resulting from increased pumping at EW-OU1-17-A could be coupled with results from the automated sample analysis system to test the hypothesis that TCE residing in the vadose zone west of the FDA is mobilized into the water table in this area by large recharge events.

Use alternate locations for treated water discharge as a simple substitute for pump tests as a flow system perturbation in future hydrologic testing at OU 1.

Modeling

Revise and update the hydrostratigraphic model as additional lithostratigraphic data become available from new wells for future flow and transport modeling studies.

Revise interpreted areas within the hydrostratigraphic model domain (where little or no lithologic data exist) as additional indirect indicators of subsurface lithology become available, such as water level responses to pumping, spatial variability in water chemistry, and geophysical surveys.

Carry out non-isothermal simulations of flow around a simulated ISPFS to evaluate apparent vertical flow and develop confidence in the estimated horizontal velocity.

Carry out additional TCE transport simulations to investigate the large dispersion observed in the model results relative to the contoured TCE plume. Consider using particle tracking methods instead of multicomponent transport to decrease numerical dispersion.

1.0 INTRODUCTION

The overall objective of this project is the development, installation, and testing of state-of-the-art sensor technologies to optimize traditional pump-and-treat remediation of contaminated groundwater. To achieve this objective, we have installed five in situ permeable flow sensors (ISPFSs) co-located with dedicated low-flow groundwater sampling pumps in the unconfined A-aquifer at a depth of approximately 100 ft (30 m) at the former Fort Ord Army Base. The site is located around the Fire Drill Area (FDA) near the Marina Airport (former Fritzsche Army Airfield), where pump-and-treat remediation has been in operation for the last 12 years. These five wells are thereby instrumented so that both velocity and chemistry can be known at nearly the same point in the same well at the same time. An additional seven existing wells were also equipped with dedicated groundwater sampling pumps. The wells in the network are connected by buried stainless steel tubing to a central onsite facility consisting of an 8 ft by 20 ft steel shipping container where gas chromatograph mass spectrometry (GCMS) is used in real time to analyze samples for volatile organic compound (VOC) chemistry. The central facility also houses a computer on which ISPFS data can be analyzed. This network of instruments can be used to monitor groundwater flow velocity and chemistry and aid in answering specific hydrologic questions that have arisen in the course of 12 years of pump-and-treat operations at OU 1. These questions include: (1) Is the FDA the source of the northwestern plume discovered in 1997? (2) How do clay bodies and flow channels affect the pump-and-treat process? (3) Why are TCE concentrations increasing at certain wells? (4) What is the impact on the GTS of infiltrating treated water within the capture zone?

A sound understanding of the subsurface hydrogeology and chemistry is critical (i) to establishing a context for interpreting data collected by the new network of instruments, (ii) to testing the new network of instrumented wells, and (iii) to addressing specific hydrologic questions. In order to develop this understanding, we have undertaken work in several different areas including: (1) detailed analysis of existing quarterly monitoring data on water table elevations and groundwater chemistry using an advanced database system; (2) construction of a three-dimensional (3D) hydrostratigraphic model and corresponding numerical grid of the A-aquifer; (3) active pump tests to perturb and monitor the flow field using ISPFSs and water level recoveries; and (4) 3D numerical simulation analyses of flow and transport using the 3D hydrostratigraphic model and associated numerical grid. An implicit objective of work in this project has been to develop experience and research infrastructure that builds upon existing knowledge and facilities. This knowledge and hydrological research infrastructure will be available for ongoing investigations of groundwater flow and transport at OU 1.

This report summarizes our work from the beginning of the project in early 1999 to the present in two sections: (1) Project Description; and (2) Results and Findings. The purpose of this structure is to separate introductory material from installation descriptions, analyses, and findings of the current project. The report is divided into sections for which various co-authors made primary contributions as follows: Daley, Sections 3, 6, and 10; Hinds, Sections 2 and 7; Jordan, Sections 4 and 8; Freifeld, Section 9; and Oldenburg, Sections 5, 11, and report preparation. Although English units are more commonly used than metric in the groundwater remediation field in the U.S., we have attempted to provide both English and metric units where practical in this report.

The breakdown of authorship defined above reflects the breakdown of effort between LBNL and LLNL. In general, LLNL was reponsible for all instrument installation and chemistry system testing, while LBNL was reponsible for data analysis and modeling, although LBNL also carried out the pump test for ISPFS testing. More specifically, LLNL was responsible for all instrument procurement, well drilling subcontracting, and instrument installation, with assistance from LBNL in network design and well placement. LLNL was further responsible for the chemical analysis system, and data collection from all instruments. LBNL developed the hydrostratigraphic model, analyzed quarterly monitoring data, carried out flow and transport simulations, and performed the pump test and ISPFS data analysis.

2.0 SITE DESCRIPTION

2.1 Location and Physical Geography

The former Fort Ord Army Base is located on Monterey Bay in northern Monterey County, California, between the cities of Salinas and Monterey (Figure 2-1). The former Fort Ord occupies the majority of a pie-shaped wedge of land bounded by Reservation Road (G17) in the north-northeast, Highway 68 in the south, and Monterey Bay in the west. The northeastern boundary of Fort Ord coincides with a 30-meter-high bluff adjacent to the Salinas River. The studies presented in this report focus on northern Fort Ord, in an area known as Operable Unit 1 (OU 1), located north of Reservation Road near the Marina Airport (former Fritzsche Army Air Field (Fritzsche AAF)). The OU 1 area, except for a rectangular 48 acre (0.2 km^2) region surrounding the FDA and groundwater treatment system (GTS), is owned and managed as a nature preserve by the University of California.

Fort Ord lies within the Coast Ranges Geomorphic Province, a region containing northwest-trending mountain ranges, broad basins, and elongate valleys that typically parallel major geologic structures such as faults within the San Andreas fault system (Tinsley, 1975; HLA, 1993). The only known major structural feature near OU 1 is the King City fault, which is part of the San Andreas fault system. The King City fault has a northwest strike, roughly coinciding with the Salinas River, and may cut through the far northeastern part of OU 1 approximately 1 mi (1.6 km) from the OU 1 GTS (HLA, 1993).

2.2 Surface Hydrology

Across the OU 1 area, elevations range from 60 to 180 feet (18 to 55 m) above mean sea level, with the highest elevation immediately southeast of the FDA (Figure 2-2). The local geomorphology is indicative of dune sands and displays hummocky topography. Highly permeable sands at the land surface readily imbibe precipitation, which averages approximately 17 in/yr (43 cm/yr) so that surface runoff is uncommon. As a result, well-developed fluvial systems are absent, while local closed basins are common (Figure 2-2). The FDA lies within one of these closed-depression drainages.

2.3 Geologic History

The shallow subsurface deposits at Fort Ord that are of interest to this study are the result of cyclical periods of sea level rise and fall over the past few hundred thousand years (e.g., Birkeland, 1972; Atwater, 1977). During this time, the Monterey Bay area has experienced marine

transgressions, resulting from periods of glacial melting and subsequent sea level rise (Tinsley, 1975). These transgressive events are separated by periods of low sea-level stands (regressions) when more of earth's water was stored in global ice masses. In the lithostratigraphic record, a transgression is indicated by a fining-upwards sequence of sediments, from fluvial gravel and sand at the bottom of the sequence to estuarine and marine clays at the top. Repetition of this pattern within a lithologic column indicates multiple periods of sea level rise and fall. Translated into a hydrogeologic context, the coarse deposits (gravels and sands) form aquifers, while the finer sediments (clays) create aquitards.

The marine-to-estuarine clays present beneath Fort Ord and also seen in the Salinas Valley represent the uppermost part of marine transgressions. These clays are collectively referred to as the Salinas Valley Aquitard (SVA), with the clays at Fort Ord often distinguished by use of a different name, the Fort Ord–Salinas Valley Aquitard (FO–SVA). The time of deposition of the clays in Salinas Valley (SVA) and those at Fort Ord (FO-SVA) is not fully understood. Peat samples from the FO–SVA have been ^{14}C- dated at over 40 kyr (Fisher et al., 1998), while Tinsley (1975) found the SVA in Salinas Valley to be of age 16–6 kyr by analysis of marine fossils. Furthermore, the top of the FO–SVA and top of the SVA are at different elevations, the FO–SVA being a few tens of feet above mean sea level, while the SVA is at or just below mean sea level (HLA, 1993).

One possible explanation for the relation between the FO-SVA and SVA is that the FO–SVA was deposited during high sea level stands between 100-130 kyr before present while the SVA is from the current modern high sea level stand, believed to have been approximately unchanged for the last 10 kyr (Harden, 1998). This is consistent with the age-dates of Fisher et al. (1998) and Tinsley (1975). The higher elevation of the FO-SVA compared to the SVA is consistent with a sea level stand for the transgression between 100-130 kyr that followed the Tahoe glaciation that is higher than the present high sea level stand (Birkeland, 1972; Harden, 1998). Under this scenario, the FO–SVA originally may have blanketed the entire Salinas Valley 100 kyr ago, but then was eroded during the Tioga glaciation (~21 kyr) as a dynamic Salinas River meandered and migrated across the valley leaving uneroded the plateau on which Fort Ord now sits. The sedimentation rate in the Salinas Valley exceeded the erosion rate throughout recent times (Tinsley, 1975), causing additional fluvial sediments to be deposited over the SVA by the Salinas River and its tributaries. In this scenario, the SVA formed in the Salinas Valley starting perhaps 15 kyr ago at approximately current sea level on top of the same sands and gravels that are present beneath the FO–SVA. Thus the FO-SVA is an erosional remnant, and because of its higher elevation was not inundated by the sea during the current sea level high stand that produced the SVA. Future research that focuses on sedimentology and

dating of the various clay layers in the FO-SVA and SVA could further elucidate the relation between the two aquicludes.

2.4 Hydrostratigraphy

The OU 1 area of Fort Ord lies within the Salinas groundwater basin. The detailed stratigraphy and hydrostratigraphy of the Salinas basin is described by HLA (1993) and is only briefly discussed here as it pertains to the current study at OU 1. Table 2-1 summarizes the geology and hydrostratigraphy in the Fort Ord area. The sedimentary materials of interest in this investigation at OU 1 are located in the shallow subsurface and primarily include the fine- to medium-grained, well-sorted older dune sands, which comprise the unconfined A-aquifer, and the underlying estuarine clay referred to as the FO–SVA. Regardless of the details of the relationship between the FO-SVA and SVA discussed above, for the purposes of the present study it is sufficient to characterize the FO-SVA as a series of clay layers separated by sands that together create an effective aquiclude between the A-aquifer and 180-foot aquifer below OU 1. Furthermore, the gradational nature of the lithological transition from mostly dune sands to clay layers separated by sands makes arbitrary the distinction between the A-aquifer and upper saturated zones within the FO-SVA. For the purposes of this study, the A-aquifer is considered to be the saturated zone above the lowest clay (Clay 1) at an elevation of approximately mean sea level.

The thickness of the sands containing the A-aquifer ranges from about 90 to 130 ft (27 to 40 m) at OU 1 due to variable topography. The present water table elevation within the A-aquifer is between 40 and 70 ft (12 and 21 m) above mean sea level (with a downward gradient to the north and northwest), making a saturated thickness of about 20 to 35 ft (6 to 11 m) within the study area (Harding ESE 2001).

Lithologic data collected during drilling activities and geophysical logging of boreholes indicate that the FO–SVA contains multiple clay layers with interbedded sands, which may reflect minor sea level oscillations or flood deposits during a single interglacial period. Based on analyses of well lithology, some FO–SVA clay layers at OU 1 appear to be laterally discontinuous, but collectively these clays may reach thicknesses of over 70 ft (21 m).

Table 2-1. Generalized geology and hydrostratigraphy at OU 1 (after HLA, 1993).

Age	Geology	Hydrostratigraphy	
Pleistocene–Holocene	Recent dune sand and alluvium	Unconfined A-aquifer	
Pleistocene	Older dune sand; sand with minor silt		
Pleistocene	Valley fill deposits	Estuarine deposits; clay with minor sand and peat	Fort Ord–Salinas Valley Aquitard (FO–SVA)
		Fluvial sand with minor gravel	Upper sandy portion of 180-foot aquifer
		Silty sand and clayey sand	Intermediate 180-foot aquitard
		Fluvial gravel and sand, with clay interbeds	Lower 180-foot aquifer
Pleistocene	Aromas Sand; eolian and fluvial sands	400-foot confined aquifer	
Plio–Pleistocene	Paso Robles Formation; alluvial fan, lake, and fluvial deposits		

2.5 Contaminant and Remediation History

Well locations at the OU 1 site adjacent to the former Fritzsche Army Airfield where ongoing investigations aimed at remediation of contaminated groundwater are shown in Figure 2-4. Historically, solvents and fuels were placed in a burn pit and used for fire fighter training in the FDA from 1962 until 1985 (HLA, 1998a) resulting in groundwater contamination consisting of volatile organic compounds (VOCs), primarily Trichloroethylene (TCE) in the unconfined A-aquifer. The burn pit was approximately 100 ft (30 m) in diameter and located in the north-central part of the currently fenced area that we refer to as the FDA. The affected area was subsequently designated Operable Unit 1 (OU 1) and the Army issued a Record of Decision (ROD) in 1988 that specified a two-phase approach to remediation. The first phase required the excavation and bioremediation of contaminated soils in the FDA. The second phase required the Army to install extraction wells as part of a GTS to remediate contaminated groundwater. Cleanup standards were set at maximum contaminant levels (MCLs). A sampling study in 1993 confirmed the

efficacy of the excavation and treatment of soils contaminated with solvents and fuels (HLA, 1994). Groundwater extraction and treatment from two wells in the A-aquifer has been underway since 1988, along with quarterly sampling for groundwater contaminant concentrations and water table elevations. In 1995, the ROD issued by the Army was signed by the Environmental Protection Agency (EPA) and California EPA (Cal/EPA).

New concern for groundwater remediation at OU 1 arose in 1997 when it was confirmed from quarterly sampling that VOCs were in groundwater downgradient from the capture area of the existing GTS (USACE, 1997; HLA, 1998a). Further investigation through installation of additional wells and monitoring have led to the delineation of a downgradient TCE plume extending 3000 ft (910 m) northwest from the presumptive source in the FDA. Currently, design and construction of an additional extraction and treatment system for the downgradient plume are underway.

OU 1 currently has approximately 70 monitoring wells and two extraction wells in operation (Figure 2-3). Extraction from wells EW-OU1-17-A and EW-OU1-18-A commenced in mid-1988 for the purpose of plume containment and remediation. Water extracted from these wells is passed through an on-site granular, activated charcoal treatment system and then pumped to the south end of the FDA where it is spread over the ground surface by a knocking head sprinkler. Both wells have been pumped at an average of approximately 8 gallons per minute (5×10^{-4} m^3/s) since the commencement of extraction, except for some short periods during which the pumping system malfunctioned or went down for maintenance. As of November 1999, the two wells had produced a total of 8.6×10^7 gallons (3.2×10^5 m^3) of water.

3.0 INTEGRATED CHEMISTRY AND FLOW MONITORING SYSTEM (ICFMS)

3.1 Remediation Site VOC Monitoring System

In numerous fields automated data collection has become commonplace for improved understanding of the primary variables that can affect complex processes. Through automated datalogging and application of multiple types of sensors, enhanced optimization becomes possible. If data can be processed and displayed in a flexible and timely fashion, system operators can both gain a more detailed understanding of the variables under their control, and respond to changes to reduce operational costs and avoid untoward failures and downtime. Generally, substitution of automated sampling and application of sensors greatly improves both the quality of data (through reduction of human errors and bias) and frequency of data collection, so short-term systematic perturbations can be detected that otherwise might be interpreted as random sampling noise. Realization of the value of automated data collection has extended into the environmental remediation disciplines, but despite extensive effort by several agencies to develop chemical sensors that could substitute for conventional sampling and laboratory analysis, sensors that offer low cost of operation, long-term in situ stability, sensitivity in the realm of low parts per billion, and selectivity to the numerous compounds usually found in contaminated groundwater have yet to be developed.

Recently, instrumentation that provides conventional compound separation and high sensitivity detection in an on-line configuration has been deployed for continuous, in-field monitoring of groundwater remediation experiments. These analytical systems have the capacity to convert the sampling of water wells into a high-frequency data acquisition application. Examples include detailed studies of in situ bioremediation processes (Hopkins et al., 1993a, 1993b; Hopkins and McCarty, 1995; McCarty et al., 1998; Roberts et al., 1990; Semprini et al., 1992), and evaluation of pulsed pumping in pump-and-treat remediation (MacKay et al., 2000). These installations took advantage of a novel flow-through sample selection and processing system, the Analytical Sampling and Analysis Platform (ASAP, A^{+}RT, Milpitas, CA, Figure 3-1). This automated device uses sample selection and flow switching valves and a unique thin-film stripping cell to process water samples and analytical standards for purge-and-trap VOC analysis under relatively unattended computer program control for prolonged periods.

We have installed one of these devices in the OU 1 Fire Drill Area monitoring facility, and augmented its configuration through integration of on-line GC control and data acquisition software developed in-house for monitoring of soil vapor extraction systems (Daley, 1992); initial testing

of this system took place at the Fort Ord OU2 Groundwater Treatment facility, and is described in greater detail in another report from this project (Task 8 - Refinement of In-Line Instrumental Analytical Tools to Evaluate their Operational Utility and Regulatory Acceptance).

The previous studies cited above have been small scale experiments that have intensively sampled relatively small zones up to only a few tens of meters in diameter. We elected to evaluate this continuous analytical system on the scale of an entire remediation site, to evaluate the practicality of installation and operation of automated long-term and on-site VOC monitoring coupled with ultra-low flow continuous sample pumping, also known as micropurging. Micropurging has been shown to have distinct advantages over conventional purge-and-sample approaches, avoiding VOC loss through surging, pressure changes, and inadvertant aeration of samples (Barcelona et al., 1994; Kearl et al., 1992, 1994; Powell and Puls, 1993; Puls et al., 1992, Robin and Gillham, 1987), yet has not been coupled with on-line analytical equipment prior to this project. The low-flow pumping and analysis system at OU 1 connects a network of wells covering a footprint of over 1000 ft (305 m), and is to our knowledge the largest system of this type assembled to date.

3.2 In Situ Permeable Flow Sensing Technology

In addition to the on-line analytical system, five newly drilled wells were installed that incorporate in situ permeable flow sensors (ISPFS, HydroTechnics, Inc.), that provide continuous estimates of groundwater flow direction and magnitude. Pressure transducers for continuous logging of water depth were also installed in all instrumented wells. The ISPFSs are a recently developed technology for measurement of groundwater flow with a tool in direct contact with the saturated formation (Ballard, 1996; Ballard et al., 1996), that avoids analytical complications associated with the presence of well casings and sand packs that hinder the interpretation of other methods for direct measurement of groundwater flow (Kearl and Case, 1992; Kerfoot and Massard, 1985). The tools comprise a cylindrical heated surface wrapped on an insulated expanded foam core, and studded with an array of precision thermistors (Figure 3-2). They are installed directly in the saturated formation by drilling beyond the intended installation depth (preferably with a hollow-stem auger or other rig that avoids use of drilling muds), lowering the tool through the auger, and then allowing the formation to collapse around the tool as the drill flights are lifted from the borehole. The surface heater dissipates up to 100 Watts of heat, warming the formation and water flowing around it. The flowing fluid advects the heat energy around the tool, cooling the upstream side, and warming the downstream. Any vertical component of flow similarly shifts the center of surface temperature away from the physical center of the tool, so both horizontal and vertical components of fluid motion can be detected. This heat transport is measured by the

thermistor array, and these raw data are collected by a datalogger installed nearby along with the heater DC power supplies. A mathematical inversion technique is incorporated into data processing software supplied by the tool manufacturer (HTFlow95; HydroTechnics, Inc., Albuquerque, NM) that estimates magnitude of horizontal and vertical flow components, flow azimuth, and other parameters as a continuous log.

We proposed that the coupled data from both chemical and physical sensing systems would provide significant improvement in understanding of the hydrology and transport properties of the OU 1 site, and provide a baseline for future experiments and modifications of extraction system operation to optimize and speed site remediation.

4.0 DATA MANAGEMENT AND ANALYSIS

4.1 Data Management System

We selected the data management system GIS\Key™ to aid in analysis of existing OU 1 data collected since 1988 by Harding ESE (nee Harding Lawson Associates (HLA)). GIS\Key™ is produced by GIS\Solutions (Walnut Creek, CA). GIS\Key™ runs on PC platforms and consists of several integrated components: (1) database, (2) query tool, (3) graphic engine, and (4) surface data manager. GIS\Key™ uses a proprietary relational data model implemented in a relational database program, which is typically Microsoft Visual FoxPro, to store environmental site data. The database can be accessed by the user through a customized FoxPro interface or through the query tool GIS Scout, a component of GIS\Key™. GIS Scout allows users to construct data queries through a simple graphical user interface. The data resulting from the query can be browsed and exported. GIS Scout can produce a number of standard regulatory reports using the query results as well. GIS Scout includes a graphics engine through which a variety of standard plots are created, such as hydrographs, total flux and mass removal plots, concentration vs. time and constituent concentration vs. constituent concentration plots, and Piper and Stiff diagrams.

GIS Scout can also send the user's query results to either Autodesk's AutoCAD™ (version 14.01 was used in this project) or ESRI's ArcView™ for creating maps of water levels, contaminant concentrations, or geologic structures, for example. Alternatively, GIS\Key™ provides custom menus within these programs for pulling geologic, hydrologic, and chemistry data from the database and posting it to a user supplied site map. The custom menu also provides for contouring this data and managing the display of investigation sites such as wells, soil sampling sites, and treatment system sampling ports, among other features.

Maps produced in AutoCAD™ can be stored using the surface data manager, or SDM, which streamlines the tracking and retrieval of map work products. The SDM stores maps as well as the data used to create a map, such as a set of water levels, the surface created from the data, such as a water table, the geographic position of the surface, and the surface metadata, such as the creation date of the surface. To retrieve a map drawing, surface, or data file the user indicates an area of interest in AutoCAD and the SDM shows a browse window with all the entities that exist at this location for user selection.

4.2 Data Transfer

GIS\Key™ includes utilities for importing data into any of the tables in the relational data structure. For quality control, these utilities perform a number of integrity checks upon records proposed for import. For instance, each utility checks for duplication of the primary key, conformance of the data fields to the GIS\Key™ field definitions, and the integrity of the relation between records proposed for import and related records in other tables. If any errors are found, the records are rejected for import, and an error report is written.

Chemistry data are typically provided by analytical laboratories and consultants in a flat file database format. This format includes a large fraction of repetitive information. For example, each record contains information on the sample, sample analysis, and analyte results, even though the analyte results are the only data unique to each record. A well-designed relational database, such as GIS\Key™, typically eliminates this redundancy, which increases data integrity and data storage and retrieval efficiency by storing the data in separate related tables. For instance, information about a particular sample, such as the source well and collection date, is stored in one record in a sample table. Each record in the sample table is related to a record(s) in an analysis table that contains information on each analysis performed on the sample, such as the type of analysis and the lab performing the analysis. Each record in the analysis table is related to a record(s) in the result table for each analyte, such as the concentration and the Practical Quantitation Limit (PQL).

GIS\Solutions provides a utility called LabBuild that transfers flat file chemistry data, such as that provided by Harding ESE for OU 1, into a number of temporary tables for import into the relevant relational chemistry data tables in the database. This utility performs the same checks mentioned above for the single table import utilities, namely primary key duplication, field conformance, and relational integrity.

Harding ESE provided approximately eight years of quarterly monitoring data that we transferred into GIS\Key™. We then used the visual interface of the data management system to abstract useful information and trends in water levels and chemistry to assist in understanding the subsurface at OU 1. While some of these trends are well known, having been previously established by Harding ESE, other observations and analyses represent new contributions to the understanding of OU 1 hydrology.

5.0 NUMERICAL SIMULATION METHODS

In general, a multiphase and multicomponent simulation capability is needed at OU 1 to model unsaturated and saturated zone flow of aqueous and gas phases containing VOCs. In this investigation, we have made use of the TOUGH2 code for 3D numerical simulation analyses (Pruess et al., 1999). TOUGH2 is a general-purpose numerical simulation program for multi-phase fluid and heat flow in porous and fractured media that can model flow and transport on irregular grids that represent realistic hydrostratigraphy. TOUGH2 uses the integral finite difference method with fully implicit time stepping and a residual formulation that is robust for coupled flow and transport problems. TOUGH is an acroynm for "Transport Of Unsaturated Groundwater and Heat," and was developed by the Earth Sciences Division of Lawrence Berkeley National Laboratory (LBNL) for applications in geothermal reservoir engineering, unsaturated zone hydrology, and contaminant hydrology, and finds application in many other fields as well. The source code for TOUGH2, written in FORTRAN77, is available from the Energy Science and Technology Software Center (ESTSC) of the U.S. Department of Energy. Further information about TOUGH2 can be found at http://www-esd.lbl.gov/TOUGH2.

With origins going back to the 1980's, the TOUGH codes have been in use for about 20 years (Pruess, 1987; Pruess, 1991). During this time, a large number of research and practical problems have been investigated using the TOUGH codes. TOUGH2 is the official code selected by the U.S. Department of Energy for its civilian nuclear waste management program to simulate flow and transport processes at the Yucca Mountain site, which is the potential repository for high-level nuclear waste. As part of the Department of Energy's Yucca Mountain Project, TOUGH2 has passed a procedure designed to ensure quality and correctness (Pruess et al., 1996). A bibliography of research reports and papers can be found at the TOUGH2 website.

TOUGH2 consists of many different modules applicable to different flow processes and systems (Pruess et al., 1999). We have made use of two different modules for work in this project: (1) EOS9; and (2) T2VOC. EOS9 is an equation of state module for water in saturated and unsaturated conditions. This module is useful for simulating unsaturated-saturated groundwater systems where the focus is on water flow as opposed to gas flow. The advantage of EOS9 is that it is a single component (water) and single-phase (aqueous) version for which simulation times are relatively fast. T2VOC is a three-phase, three-component module of TOUGH2 that models two liquid phases (e.g., nonaqueous phase liquid and water) as well as a gas phase, along with three chemical components (i.e., water, VOC, and air) (Falta et al. (1992a, b; 1995)). T2VOC is capable of simulating a range of systems from the very complex (e.g., steam flooding remediation involving nonaqueous phase liquids (NAPLs) where heat volatilizes VOC and removes it in the gas phase) to simple (e.g., low concentration

contaminants in the aqueous phase). Although TOUGH2 is capable of more complex processes, the focus in this project is on isothermal groundwater flow in the saturated zone, along with transport of dissolved VOC at low concentrations.

6.0 INSTALLATION OF INTEGRATED CHEMICAL AND FLOW MONITORING SYSTEM (ICFMS)

6.1 In Situ Permeable Flow Sensors

Locations for installation of five new wells that were to include ISPFSs were chosen based on an existing flow field model that addressed the flow channels created by the groundwater extraction system pumping on EW-OU1-17-A and EW-OU1-18-A (Harding Lawson Associates (HLA), 1998b; Figure 6-1). Three of the wells, MW-OU1-36-A, MW-OU1-37-A, and MW-OU1-38-A, were sited to transect the extraction contours predicted to separate paths to the two extraction wells; well MW-OU1-38-A also provided an additional sampling point expected to lie outside the 1 ppb contour of TCE drawn from 1998 monitoring data, and to be relatively free of VOCs. MW-OU1-39-A was sited in a location expected to show a significant change in flow direction if either of the extraction wells was either shut off or pulsed. Finally, MW-OU1-40-A was located to provide a flow monitoring location well away from the predicted influence of the extraction wells, that might shed light on the flow conditions near the upgradient portion of the "northern" portion of the OU1 plume.

The ISPFs have an upper limit of approximately 400 ft (122 m) between the sensors themselves and their respective power supplies. Accordingly, weather-tight, ventilated steel boxes were located in two central positions to house the supplies and dataloggers (Figure 6-2). At this point the additional five pre-existing wells to be instrumented with sampling pumps and pressure transducers were selected. These included MW-OU1-05-A and MW-OU1-19-A, located in a portion of the plume where TCE concentrations had been rising in recent quarters (D. Eisen, USACE, personal communication), MW-OU1-04-A and MW-OU1-07-A, which were thought to be well located for future tracer experiments to characterize the extraction-induced flow field, and MW-OU1-20-A, located just at the edge of the modeled flow field, and centered in the isthmus between the FDA plume and the northern plume areas. The initial proposed routes for interconnecting sample lines are shown in Figure 6-2.

The five new wells were drilled in August 1999. A field engineer and hydrogeologist from the ISPFS manufacturer (Dave Wardwell, HydroTechnics, Inc.) supervised the installation of the flow sensors, and conducted initial testing to ensure operation. Boreholes were drilled with 12 in (30 cm) diameter hollow-stem augers until the FO-SVA clays were reached at depths of 90 to 124 ft (27.4 to 37.8 m). Logs of the wells, and a schematic of the parallel ISPFSs and monitoring well completions are illustrated in Figures 6-3 through 6-19.

Planning for the locating of wells and ancillary equipment took place in Spring 1998, just following the high rainfall El Niño year of 1997-1998.

During that season, surveys of the rare plant species *Gilia tenuiflora* ssp. *Arenaria* (sand gilia) and Chorizanthe p. pungens (Monterey spineflower) found these plants well distributed over the site, and in virtually all the areas identified for installation of sampling equipment, transfer lines and signal cabling (Figure 6-20). In order that the work at the site adhere to the CERCLA requirement that remedial actions be conducted in a manner that meets applicable or relevant and appropriate requirements (ARARs) of state and federal laws, Biological Clearances were prepared by staff biologists at Harding Lawson Associates (now Harding ESE) that offered guidance for methods of well drilling and equipment installation that would be compatible with preservation of the ecological resources at the site as managed by the University of California, Natural Reserve System (UC/NRS).

Additional plant surveys were conducted prior to the drilling operations in August, 1999 that found much reduced distributions of the threatened (*Chorizanthe*) and endangered (*Gilia*) species. Discussions with the managers of the UC/NRS reserve identified elevated concern over the possible long-term damage above-ground conduit might pose to the ecological resources at the site, and that construction during the growing season of would be detrimental to conservation efforts. Consequently, trenching for permanent installation of sampling plumbing and sensor cabling was postponed until the end of the Spring 2000 growing season. Additionally, in order to avoid possibly compromising portions of the habitat with the presence of above-ground equipment, we elected to bury all interconnecting lines in electrical-grade CPVC conduit, following the guidelines set out in the Biological Clearance.

Conduit excavation was performed with a four-wheel drive trencher (Ditch-Witch, Inc.) and hand tools, after we determined that smaller walk-behind equipment foundered in the loose surface sands of the site. At all locations outside the FDA where populations of rare plant species might be present, surface soil was manually windrowed onto plastic sheeting laid parallel to the trenches, for redistribution following equipment installation (Figure 6-21, top left).

At each instrumented wellhead, a weather-tight "transfer box" was installed to house the solar-electric bladder pump controllers (C100, QED Environmental, Inc.), incoming air lines, returning stainless steel groundwater sample lines, and signal cables for the ISPFSs and pressure transducers (Figure 6-21, top right, and center left). The pump controllers required only dry compressed air and a small solar cell mounted on each transfer box to operate the pumps; programming of the fill and discharge cycles of each pump was performed on a keypad on the front of each controller (Figure 6-21, center right). At the new wells, 1 in (2.54 cm) conduit mounted flush to the ground surface provided protection for air, water and signal connections to the well caps (Figure 6-21, center left); at pre-existing wells a goose-neck of 1 in (2.54 cm) galvanized conduit was

used (Figure 6-21, top right). The pumps installed were of all Teflon® and stainless steel construction (T1100M MicroPurge® bladder pumps, QED Environmental, Inc.). Returning water lines from the pumps to the surface, and to the monitoring instrument facility were 1/4 in (0.635 cm) O.D., annealed, stainless steel tubing (American Tubing, Inc.); this material was sufficiently malleable that it could be pulled through conduit along with air and signal lines. Two ground-flush junction boxes and six pull boxes were installed approximately every 200–300 ft (61–91 m) to ease pulling in the line bundles. All plumbing line unions and signal junctions were made in these vaults; no unions were used in any conduit runs, to ensure future maintenance access. The final layout of all conduit is shown in Figure 6-22.

Following modification of the supplied datalogger code for control of the ISPFSs to add water depth recording, datalogging was started for MW-OU1-36-A, MW-OU1-37-A and MW-OU1-38-A on September 30, 2000, followed by MW-OU1-39-A and MW-OU1-40-A on October 5, 2000. Logging has continued since that time, and is discussed further below; power outages interrupted data collection for a total of eight days since logging startup.

6.2 Realtime Chemical Analysis System

The ASAP water sampler and gas chromatograph are housed in a steel transportation container outfitted as a field laboratory. As with other installations of this equipment, the building is equipped with air conditioners and heating to maintain a relatively constant temperature of 23 C. All 1/4 in (0.635 cm) sample lines from instrumented wells emerge into an outdoor vault ("Junction Box 1," Figure 6-22), where they are fed into the building and to the ASAP. Each line terminates in a "T," one arm of which connects to the primary sample selection valve on the ASAP (Figure 6-23, Item 15); the other directs flow to one of a bank of flowmeters mounted above the ASAP. In this way, all bladder pumps could be operated continuously, and between adjustment of their fill and delivery cycle times programmed at the wellhead controllers, and needle valves at the rotameters, a continuous stream of sample water is supplied at approximately 150 mL/min. At the moment a sample was selected for analysis, only the short lengths of tubing between the "Ts" and the selection valves need to be flushed to acquire a representative sample.

At the point when a sample is taken for analysis, the primary sample selection valve is moved to select from one of the twelve incoming streams (at this time, two additional sample ports have been reserved for EW-OU1-17-A and EW-OU1-18-A extraction well lines, but not yet attached to the system). The sample pump and solenoid are actuated, to flush a VOA vial on the off-line sampling rack, through the secondary sample valve. Flushing produces a headspace-free sample that can be

collected for tracer or other analysis; flushing time is operator programmable.

Following the VOA vial flush, the sample pump solenoid closes, and the sample flows through 1/16 in (0.159 cm) sample loops and valves in the liquid processing module. Following a flushing interval, the sample is pushed back through the liquid process valve (Item 10) by a stream of bubbles generated by the blank rinse peristaltic pump. The bubbles ensure that droplets do not adhere to tubing walls. VOCs are swept from the sample as it flows through the thin-film stripping cell by a counter-current flow of helium, to the trap in the gas trapping module (Item 3). The trap is a commercially packed three-component sorbent bed in a 1/8 in (0.32 cm) x 30 cm tube (Carbopack™-B and Carbosieve™ S-III , Style "8" for Model 2000 purge-and-trap; Tekmar-Dohrmann, Inc.) Following a dry-purge cycle, during which dry helium flows through the trap (in the direction of sample application) to remove moisture, the trap is isolated from carrier gas flow, heated to the desorbtion temperature of 215 C, then the carrier flow direction is switched, to flush VOCs from the trap to the gas chromatograph for compound separation and detection.

In this installation a capillary gas chromatograph (GC, SRI Instruments, Torrance, CA) was outfitted with a dry elecrtrolytic conductivity detector (SRI), and an RTX-502.2 capillary column (60 m x 0.32 mm I.D., 1.8μm thick film; Restek©, Bellefonte, PA). Control of the GC column pressure and oven temperature, and acquisition of detector signals were performed with a custom application developed in LabVIEW (LabVIEW version 6i, National Instrument, Austin, TX). Raw detector signals were saved on disk as binary files in the native format of the Igor plotting software package (version 4.0.2, Wavemetrics, Lake Oswego, OR) for display or quantitation with additional software modules written in LabVIEW. Software was run on a rack mounted Apple PowerMac 9600 equipped with a PC emulation board (OrangeMicro, Anaheim, CA), used for collection of flow sensor datalogger files, and for low-level programming of the ASAP embedded controller.

Calibration of the ASAP/GC was performed prior to each set of well samples by analyzing up to six samples from two custom gas-tight syringes mounted on the ASAP. The syringes were filled with ultra-high purity water from the carbon filter and counter-current helium stripping subsystem that supplied rinse water to the ASAP (Figure 1.3-1, Item 4), and spiked with either 20 or 250 μL of a commercially prepared VOC standard (CLP-150, Ultra Scientific, Kingstown, RI). Compound identification was achieved by comparison of chromatograms with vendor-supplied plots, and injection of single compounds, as necessary. A typical standard run is shown in Figure 6-23.

7.0 HYDROSTRATIGRAPHIC MODEL DEVELOPMENT

7.1 Data Sources

The hydrostratigraphic model developed for OU 1 is a simplified, three-dimensional representation of subsurface lithologic variability believed to have an impact on groundwater movement through the unsaturated zone and within the shallow A-aquifer. The hydrostratigraphic model is the basis for generating the numerical grid used with TOUGH2 to simulate and evaluate the flow and contaminant transport behavior at OU1.

Development of a hydrostratigraphic model began with the compilation of data describing well locations, lithology (from well logs), and land surface features, such as topography and location of the presumed contaminant source. A model domain was established based on available hydrostratigraphic data, water chemistry data (defining the lateral extent of the contaminant plume), and the general position of the shallow A-aquifer. The resulting model covers an area of 0.34 mi^2 (0.87 km^2) as shown in Figure 7-1. The top of the hydrostratigraphic model coincides with the land surface, which is 94 to 177 ft (28 to 54 m) above mean sea level (msl) within the model domain. The bottom model boundary is mean sea level.

Well data and topographic information used to develop the hydrostratigraphic model were provided by Harding ESE. The well data consist of paper copies of field logs and surveyed easting and northing coordinates. Table 7-1 lists 70 wells used in the development of the hydrostratigraphic model and their locations.

Table 7-1. Location (NAD83 Coordinates, in ft) of 70 wells used to develop the hydrostratigraphic model of OU 1.

WELL ID	EASTING (ft)	NORTHING (ft)	WELL ID	EASTING (ft)	NORTHING (ft)
MW-OU1-01-A	5748528.4	2142460.9	MW-OU1-37-A	5748592.8	2142800.5
MW-OU1-02-A	5748933.5	2142535.2	MW-OU1-38-A	5748835.5	2142942.5
MW-OU1-03-A	5748664.0	2142992.2	MW-OU1-39-A	5748487.9	2143120.6
MW-OU1-04-A	5748321.2	2143134.7	MW-OU1-40-A	5748720.9	2143606.8
MW-OU1-05-A	5748140.3	2142926.2	MW-40-01-A	5749953.3	2143052.3
MW-OU1-06-A	5748304.5	2142588.3	PB-BW-11	5748926.3	2142970.1
MW-OU1-07-A	5748467.0	2142826.4	PB-BW-12	5748375.0	2142200.0
MW-OU1-08-A	5748686.6	2143320.8	PB-BW-13	5748782.0	2142188.0
MW-OU1-09-A	5747971.3	2143341.8	MW-BW-10-A	5748531.6	2142152.7
MW-OU1-10-A	5748115.7	2143291.6	MW-B-05-180	5749043.1	2144750.4
MW-OU1-11-SVA	5748621.2	2143027.9	MW-B-06-180	5749001.0	2144822.8
MW-OU1-12-A	5748539.7	2142779.7	HP-OU1-15	5747657.1	2144629.2
PZ-OU1-13-A	5748278.8	2143296.1	HP-OU1-16	5748113.1	2144847.0
PZ-OU1-14-A	5748261.5	2143276.2	HP-OU1-17	5748617.2	2144405.1
PZ-OU1-15-A	5748607.3	2142964.3	HP-OU1-18	5749610.4	2144709.9
MW-OU1-16-A	5748593.5	2142996.6	HP-OU1-20	5749742.5	2143666.7
EW-OU1-17-A	5748275.3	2143274.4	HP-OU1-21	5749941.9	2143429.1
EW-OU1-18-A	5748613.3	2142977.3	HP-OU1-22	5749597.4	2143332.5
MW-OU1-19-A	5748128.8	2143102.9	HP-OU1-24	5747359.2	2145011.9
MW-OU1-20-A	5748507.8	2143396.9	HP-OU1-27	5747318.0	2144668.2
MW-OU1-21-A	5748991.1	2143797.6	HP-OU1-28	5747844.5	2142793.5
MW-OU1-22-A	5748441.6	2143981.1	FAA-HP-1	5749321.5	2143207.6
MW-OU1-23-A	5748415.9	2143573.7	FAA-HP-2	5749134.1	2143455.3
MW-OU1-24-A	5747442.5	2143915.0	FAA-HP-3	5748848.1	2143566.0
MW-OU1-25-A	5748103.2	2143613.5	FAA-HP-4	5748652.7	2143687.3
MW-OU1-26-A	5747960.0	2144141.8	FAA-HP-5	5748449.5	2143959.4
MW-OU1-27-A	5747460.4	2144578.1	FAA-HP-6	5748299.6	2144170.4
MW-OU1-28-A	5747957.3	2144664.4	FAA-HP-7	5748900.5	2144154.0
MW-OU1-29-A	5747644.8	2144665.0	FAA-HP-8	5749188.5	2144095.6
MW-OU1-30-A	5748515.7	2144371.4	FAA-HP-9	5748049.3	2144537.1
PZ-OU1-31-A	5749040.6	2144653.9	FAA-HP-10	5748937.9	2144526.7
MW-OU1-32-A	5748827.0	2143487.3	FAA-HP-11	5749450.4	2143916.4
MW-OU1-34-A	5747498.3	2144837.6	MW-OU1-01-180	5748523.8	2142672.1
PZ-OU1-35-A	5747615.8	2144655.8	MW-OU1-02-180	5748430.6	2142159.5
MW-OU1-36-A	5748447.8	2142671.1	MW-OU1-03-180	5749357.6	2142836.7

7.2 Data Limitations and Uncertainties

Data constraining clay and sand occurrence at depth are very limited, since most wells terminate within the first few feet of the first clay layer encountered. However, the deeper wells (e.g., MW-OU1-11-SVA, MW-OU1-01-180, MW-OU1-02-180, MW-OU1-03-180, MW-B-05-180, MW-

B-06-180), along with a few of the shallower wells (e.g., MW-OU1-12-A, MW-OU1-32/33-A), indicate the presence of multiple clay layers between the A-aquifer and the 180-foot aquifer.

The variety of drilling and logging methods used have inherent limitations. In most cases, wells were logged using cuttings, an approach that prevents the determination of the exact depth to stratigraphic boundaries due to the mixing of sediments from different vertical locations. Approximately 10 wells were logged by coring, which provides better depth control when identifying layer contacts and avoids mixing of sediments. However, heaving sands are often problematic during drilling when approaching the FO-SVA, which can skew measurements of depth to layer contacts. Geophysical logs were available for 4 wells. Typically, this is a reliable approach for mapping layer contacts; however, transitional sandy clays sometimes effectively mask the geophysical signature of the clay. For development of the hydrostratigraphic model, geophysical logs were assumed to be the most reliable, followed by core, and then cuttings.

A further complication exists because different log types within a given well may not yield consistent information about layer contacts. For instance, MW-OU1-01-180, MW-OU1-02-180, MW-OU1-03-180, and MW-OU1-11-SVA have been logged using both cuttings and geophysical methods. A comparison of the results shows inconsistencies in layer elevations of more than a meter.

FO-SVA-clay data from the OU 1 area were logged by more than a dozen geologists over a span of about 15 years (1985–2000). The logs contain variable amounts of information including soil color (using a Munsell chart), grain size (clay, silt, sand, gravel) and percent, soil classification (e.g., CL, CH, SP, etc.), consistency/relative density, and moisture of the sediments encountered.

We undertook an analysis of clay color/classification (recorded on well logs) in an attempt to differentiate between potentially distinct clay bodies at the OU 1 site (e.g., Smedes et al., 1993). The clay colors observed include: olive gray, gray, olive, olive brown, grayish brown, bluish gray, dark greenish gray, and yellowish brown. Occurrence of these colors does not appear to be restricted to a certain elevation or stratigraphic position. However, in some instances, there appear to be local trends, where a grouping of wells contains clays of the same color at approximately the same elevation. In general the results were inconclusive; clear spatial correlations could not be established based on observed clay characteristics from field logs. Thus, no distinction among clays exists in the hydrostratigraphic model.

7.3 Model Development

Although variable mixtures of sand, silt, and clay occur in the subsurface at OU 1, the only lithologies represented in the hydrostratigraphic model are sand and clay. As a general rule, silty sand, sandy silt, and silt are represented as sand in the hydrostratigraphic model, while clayey sand, clayey silt, silty clay, and sandy clay are represented as clay. Sediments identified in the well logs are typically either sand or clay.

An eight-layer model of alternating sand and clay (4 sand layers, 4 clay layers) was developed to represent the subsurface hydrostratigraphy of OU 1. Not all layers are continuous across the model domain because of the transgressive/regressive nature of the deposits, which create wedges of sediment with pinch-out margins. A cross section illustrating the layering approach used in the hydrostratigraphic model is shown in Figure 7-2. No internal sedimentary characteristics distinguish one sand layer (or clay layer) from another. In other words, we assume all sand layers to have the same characteristics (likewise for the clay layers). The number of layers used in the model is somewhat arbitrary. We attempt to strike a balance between the available data and the presumed subsurface variability. Overall, the approach used allows for representation of discrete, discontinuous clay layers.

The model is built by stacking layer thicknesses (isochores) on top of a reference horizon. The reference horizon in this hydrostratigraphic model is mean sea level. Thickness maps are developed for each model layer (i.e., 4 clay layers and 4 sand layers) based on data contained in the well logs, along with some interpretive constraints.

7.4 Layer Geometries

Clay 1 and Clay 2 are both continuous across the model domain. Clay 3 and Clay 4 (hereafter referred to as the Airfield Clay) are both discontinuous, with Clay 3 occurring in the southeast quadrant of the model domain and the Airfield Clay typically present in the southern half of the model domain (see Figure 7-3a, b).

Clay 1 is the lowest layer in the hydrostratigraphic model and has about 1.5 to 9 ft (0.46 to 2.7 m) of thickness. Wells used to constrain the thickness of Clay 1 are MW-OU1-01-180, MW-OU1-02-180, MW-OU1-03-180, MW-OU1-11-SVA, MW-B-05-180, and MW-B-06-180. For other locations in the OU1 area, a mean thickness of 3 ft (0.91 m) was used for Clay 1.

Clay 2 is the second clay from the bottom in the hydrostratigraphic model and ranges in thickness from about 2 to 10.5 ft (0.61 to 3.2 m), with a mean thickness of 5.2 ft (1.6 m). The top of Clay 2 occurs at an elevation of about 15 to 30 ft (4.6 to 9.1 m) above msl. The elevation of the top of Clay 2 is constrained by approximately 40 wells; however, the thickness of Clay 2 is poorly constrained since almost none of these wells

completely penetrate the layer (an average value of about 5 ft (1.5 m) was assigned in most places based on minimal thickesses observed in well logs).

Clay 3 is the third clay from the bottom in the hydrostratigraphic model and ranges in thickness from 0 to 12 ft (0 to 3.7 m). Where present, the top of Clay 3 occurs at an elevation of about 30 to 40 ft (9.1 to 12.2 m) above msl. The elevation of the top of Clay 3 is constrained by approximately 20 wells. Clay 3 thicknesses are inferred from very limited well data.

The Airfield Clay is the highest clay in the hydrostratigraphic model and ranges in thickness from 0 to 10 ft (0 to 3.0 m). Where present, the top of the Airfield Clay occurs at an elevation of about 35 to 50 ft (10.7 to 15.2 m) above msl. The elevation of the top of the Airfield Clay is constrained by 11 wells. Thicknesses are known from about half of the well logs and are inferred from the other half.

Sand 1 (except at well MW-B-05-180) and Sand 4 are both continuous across the model domain. Sand 2 and Sand 3 are both discontinuous, with Sand 2 pinching out mainly in the southern half of the model domain (but also locally in the northeast) and Sand 3 pinching out in the southeast corner of the model domain.

Sand 1 is the lowest sand layer in the hydrostratigraphic model (situated between Clays 1 and 2) and has a mean thickness of 15 ft (4.6 m) (maximum: 22 ft (6.7 m)). Sand 2 lies between Clays 2 and 3 and has a mean thickness of 5.5 ft (1.7 m) (maximum: 15 ft (4.6 m)). Sand 3 occurs between Clays 3 and 4 and has a mean thickness of 8 ft (2.4 m) (maximum: 10.6 ft (3.2 m)). Sand 4 is the uppermost layer of the hydrostratigraphic model and has a mean thickness of 92 ft (28.0 m) (range: 54 to 133 ft (16.5 to 40.5 m)).

8.0 WATER LEVEL AND CONTAMINANT CHEMISTRY DATA ANALYSIS

8.1 OU 1 Site Data Transfer

Harding ESE provided site maps and well location, water level, and groundwater chemistry data relevant to OU 1. The OU 1 site maps were in drawing exchange file (dxf) format. One site map was provided with topographic information and another site map contained all of the other site information. LBNL separated the entities in each of these drawings into additional layers to allow more flexibility in map creation. The resulting drawings were merged into one AutoCAD site map, some of whose layers are shown on Figure 8-1. This figure also shows all the sample sites for which water data were provided. Water level data were provided for the extraction wells from July 1993 to December 2000, for the MW-B monitoring wells from January 1992 to December 2000, and from the MW-OU1 monitoring wells from June 1988 to December 2000. The groundwater chemistry data included analytical results from samples collected from monitoring wells from April 1992 to March 2000, and from the groundwater treatment system from July 1993 to March 2000. Wells MW-OU1-41-A to MW-OU1-44-A were installed too recently to provide meaningful data, and therefore were not included in the following analyses.

Harding ESE provided the sample site data as delimited text and paper well logs. LBNL combined this sample site information into one delimited text file containing information on sample site name, type, and position. For some sample sites, the position and ground surface elevation were taken or interpolated from the site map. The sample site file was imported into GIS\Key™ via an import utility to store sample sites in the database. The sample site symbols on the base map contain links to the database for mapping purposes.

The location of the sample sites imported from GIS\Key™ were compared to those included originally on the base map by Harding ESE. The locations of four sample sites were found to be different, as shown in Table 8-1. As the differences were not great, particularly for the monitoring wells, the positions of the sample sites imported into the database were accepted for the purposes of this study.

Table 8-1. Absolute distances between imported and base map sample sites.

Sample Site	Distance (feet)	Distance (m)
PB-BW-12	100	30.5
PB-BW-13	32	9.7
MW-BW-10-A	25	7.6
MW-B-12-A	25	7.6

Harding ESE provided the water level and chemistry data in delimited text and spreadsheet format. These files contained the Harding ESE data fields most analogous to GIS\Key™ data fields based upon our prior communication with Harding ESE. The OU 1 water level data file was imported into GIS\Key™ using an import utility after minor reformatting of the original data file into a GIS\Key™ compliant format.

For ease of transfer, the chemistry data file provided by Harding ESE was exported from their internal relational database to a delimited text file. The Harding ESE OU 1 chemistry file had to be edited for a number of reasons prior to entry into the database. For example, soil, soil gas, and field parameter results were removed as they are beyond the scope of the current project. Some site names were changed for clarity: TS-OU1-INF-1 was changed to EW-OU1-17-A, TS-OU1-INF-2 was changed to EW-OU1-18-A, and MW-OU1-31-A was changed to PZ-OU1-31-A. The laboratory and expert review code fields were removed due to incomplete information regarding the meanings of the codes used in these fields. A review code flagging concentrations reported below the PQL was created. The fields were changed into GIS\Key™ compliant fields by altering some field formats and recoding values in some of the fields. Finally, some new GIS\Key™-required fields were calculated based upon values in Harding ESE fields. Other GIS\Key™-required fields were included with constant values. The file resulting from these efforts was sent through LabBuild.

Based upon the automatic checks performed by LabBuild, some further manual alterations to the file and the database were made to allow import. In reformatting the file, it was assumed there was only one primary water sample per site per day. As multiple primary water samples were in fact taken on the same day in some instances, LabBuild reported the presence of some duplicate samples in the file. To resolve this error, samples in the "duplicate" sample set were arbitrarily assigned as primary sample 1, primary sample 2, etc. as needed. In one instance, examination of the laboratory method of identification indicated that a sample was in fact probably a duplicate even though the Harding ESE field sample type indicated it was a primary sample. The corrections employed to resolve these errors did not significantly affect the subsequent data analysis as all of the results involved were non-detect except for the treatment system effluent.

In its automatic comparing of the chemical names and CAS numbers in the file proposed for import against those already contained in the GIS\Key™ database, LabBuild detected numerous unknown chemical names and CAS numbers in the OU 1 chemistry file. The unrecognized chemicals names and CAS numbers were some of the inorganic analytes and various total hydrocarbons. These conflicts were resolved by adding new chemical name aliases to some of the CAS numbers in GIS\Key™, or new chemical names and CAS numbers to GIS\Key™ as warranted. The latter was done only for three alkalinity and three total hydrocarbon measurements. The corrections employed to resolve chemical name and CAS number errors did not significantly affect the subsequent data analysis as the alkalinity types added are not used for any standard inorganic constituent plots, such as Piper or Stiff diagrams, and no analysis of the total hydrocarbon data was performed due to the lack of any significant total hydrocarbons at the site.

8.2 Precipitation

Monthly precipitation totals from 1960 to 2000 were downloaded from the National Oceanic and Atmospheric Administration (NOAA) data server for the Monterey and Salinas No. 2 stations. Data from Fritzsche AAF were available only for the years 1969 to 1978. The monthly precipitation totals were summed to hydrologic year (July 1 to June 30) totals as shown on Figure 8-2. In this report the hydrologic year will be referred to by the year in which January 1 occurs. Therefore the hydrologic year beginning July 1, 1969, and ending June 30, 1970, will be referred to as the 1970 hydrologic year.

The annual precipitation totals are plotted in Figure 8-2. The 1986, 1987 and 1990 hydrologic year precipitation totals are missing for Salinas No. 2 due to missing monthly totals within those hydrologic years. Figure 8-2 shows that the hydrologic year precipitation totals at Fritzsche AAF and Salinas No. 2 match fairly well and are both somewhat less than the totals at Monterey. The Fritzsche AAF totals are 6% less and 22% less than the Salinas No. 2 and the Monterey totals, respectively, as shown on Table 8-2. While the Salinas No. 2 totals are closer to the Fritzsche AAF totals than are the Monterey totals, the Monterey totals will be used as a baseline to estimate OU 1 precipitation due to the missing Salinas No. 2 totals from several recent years.

Table 8-2. Comparison of precipitation totals.

hydrologic year	Fritzsche AAF total (inches)	Salinas No 2 total (inches)	Fritzsche AAF/ Salinas No 2 as %	Monterey total (inches)	Fritzsche AAF /Monterey as %
1969	24.87	23.36	106.5%	28.36	87.7%
1970	12.92	14.97	86.3%	16.08	80.3%
1971	14.21	13.14	108.1%	17.45	81.4%
1972	6.06	7.29	83.1%	10.9	55.6%
1973	20.61	23.34	88.3%	27.35	75.4%
1974	23.21	22.84	101.6%	24.13	96.2%
1975	12.81	14.07	91.0%	15.82	81.0%
1976	6.49	7.55	86.0%	9.86	65.8%
1977	8.6	9.11	94.4%	10.46	82.2%
1978	20.71	21.79	95.0%	29.56	70.1%
average	15.05	15.75	94.0%	19.00	77.6%

The average annual precipitation at the Monterey station from hydrologic year 1965, the beginning of the continuous data record, to 2000 is 20.6 inches. The average annual precipitation at the Monterey station from the hydrologic year 1989, which is the beginning of the OU 1 water level data provided by Harding ESE, to 2000 is 22.0 inches (55.9 cm). Using the ratios provided in Table 8-2 to adjust these Monterey station average totals to Fritzsche AAF average totals yields a 1965 to 2000 average of 16.0 inches (40.6 cm) and a 1989 to 2000 average total of 17.1 inches (43.4 cm).

The 1998 hydrologic year total is significant within the recent rainfall record. The total precipitation at the Monterey station during 1998 was 47.15 inches (119.8 cm), which is more than twice the average total annual precipitation at this station. The 1998 total was the largest annual total in the last 40 years at Monterey station, and 55% greater than the next closest total during the previous fourteen years. The 1998 hydrologic year total was also the largest in the last 40 years at the Salinas No. 2 station. The heavy precipitation in 1998 will be shown below to have had a measurable effect on groundwater levels and contaminant transport at OU 1.

8.3 Hydrologic Setting Overview

As explained in Section 2.4, the A-aquifer lies unconfined in sands above the interlayered estuarine and tidal marsh clays and sands of the FO-SVA. The FO-SVA separates the A-aquifer from the alluvial gravels and sands of the 180-ft aquifer. Some of the clay layers appear to be quite extensive while others exist over only a small portion of the FO-SVA. As shown in Figure 7-2, the upper part of the FO-SVA in the OU 1 area consists of two deeper geographically extensive clays designated Clay 1 and Clay 2, which are separated by Sand 1. These are overlain by Sand 2. Sand 3 and

4 are separated from Sand 2 and each other by geographically restricted Clay 3 and Airfield Clay.

8.4 A-Aquifer Hydrology

The water levels in the A-aquifer around OU 1 range from 8 to 76 ft (2.4 to 23 m) amsl. Water levels in this aquifer generally respond to annual precipitation as indicated by annual rises typically of 1 ft (0.30 m) or less in most wells and by the 6–10 ft (1.8–3.0 m) rise during and after the 1998 hydrologic year. Figure 8-3 is a hydrograph showing these features. The water level rises following the 1998 precipitation events are clearly exceptional. The hydrographs indicate that in 2000 the water levels in the A-aquifer at OU 1 were generally near the post-1998 maximum with the water levels in most wells in the OU 1 plume area still rising two years and more after the large 1998 hydrologic year storms.

The April to June (second quarter) 2000 water levels in wells screened in the unconfined A-aquifer are shown contoured on Figures 8-4 and 8-5. This quarter was selected for analysis because there were no transients in either of the extraction wells at the time (the relevance of which is explained below in Section 8.9), and the set of water levels from this quarter contained the fewest outlying measurements based upon examination of each well's hydrograph. Substitute data are shown on Figures 8-4 and 8-5 as follows due to outlying measurements for the following wells: the July to September (third quarter) 2000 measurements are shown for MW-OU1-07-A and MW-OU1-20-A, and the October to December (fourth quarter) 2000 measurement is shown for MW-OU1-37-A.

The water levels on Figures 8-4 and 8-5, as well as the rest of the water level maps generated from Harding ESE data, were machine gridded and contoured to generate the water tables shown. This process produces artifacts not representative of the actual water table, but overall the contours provide a reasonable water table representation that shows a number of prominent hydrologic features. Specifically, the area of apparent water table depression due to extraction extends to the northwest of EW-OU1-17-A and EW-OU1-18-A. Treated groundwater is sprinkled on the ground surface near the southern part of the fenced FDA. Mounding of the water table beneath the sprinkler recharge area is evident at this location in Figure 8-5. The boundaries of Clay 3 and 4 are shown in the figures by wide blue and yellow lines, respectively. The largest gradients in the study area are present at the edge of the Airfield Clay, presumably due at least in part to reduced transmissivity resulting from thinning of the saturated zone toward the edge.

The water table gradient in the study area varies from 0.004 to 0.04. The gradient is 0.021 in the FDA and increases to 0.033 toward EW-OU1-17-A. The gradient across the edge of the Airfield Clay near EW-OU1-17-A

is 0.041. The gradient to the north of OU 1 is 0.004, to the east and south is 0.005, and to the west is 0.011. The gradient near the edge of the FO-SVA to the west of OU 1 is 0.020. The average hydraulic gradient in the FDA, as taken from just upgradient of the water table mounding due to sprinkler recharge, to just downgradient of the Airfield Clay is 0.012. To put these numbers in perspective, using an average hydraulic conductivity of 1.8×10^{-5} m/s (see Section 9.2) and generalized gradient of 0.012, we obtain a Darcy velocity of 0.061 ft/day (2.2×10^{-7} m/s). Assuming an effective porosity of 30%, the average pore velocity is 0.20 ft/day (7.2×10^{-7} m/s). For a well spacing of 100 feet (30 m), interwell tracer transport would take on the order of 450 days. This points to the need for long term monitoring if tracer tests are undertaken at OU 1.

8.5 FO-SVA Hydrology

There are two wells screened exclusively within sandy interbeds in the FO-SVA: MW-OU1-33-A and MW-OU1-11-SVA. This is an insufficient number of wells to determine gradients within the FO-SVA sandy interlayers, hereafter referred to as aquifers, but these wells do allow some understanding of vertical gradients through the FO-SVA.

MW-OU1-33-A is screened within Sands 2 and 3, which appear to have no clay separating them at this location, and below the Airfield Clay. The water level in this well indicates that the lower sandy (Sand 2/3) aquifer is confined at this location with a groundwater potential 18 ft (5.5 m) above the base of the airfield clay at the end of 2000. Throughout 2000, the water level in this well was 5 ft (1.5 m) lower than the water level in well MW-OU1-32-A, which is screened in Sand 4 above the Airfield Clay. This head difference equates to a downward vertical gradient of 1.0 using a vertical distance of 5 ft (1.5 m) between the top and bottom of the Airfield Clay at this location. The annual water level variation in this well is unknown due to the short duration of the water level record.

The Sand 2/3 aquifer appears to transition from confined beneath the Airfield Clay to unconfined where Airfield Clay is absent. A second quarter, 2000 piezometric map using the sub-Airfield Clay water level from MW-OU1-33-A in place of the supra-Airfield Clay water levels from MW-OU1-08-A, MW-OU1-20-A, MW-OU1-32-A, MW-OU1-39-A is shown on Figure 8-6. The difference in the water levels between MW-OU1-33-A and MW-OU1-40-A, which are both screened in Sand 2/3, suggests these wells are not hydrologically connected. The groundwater potential beneath the Airfield Clay is almost the same as around extraction well EW-OU1-17-A suggesting the unconfined groundwater "cascading" off the edge of the Airfield Clay may flow under the Airfield Clay as well as toward the extraction well.

MW-OU1-11-SVA is screened across three sand layers, the uppermost of which is Sand 1, which is separated throughout the study area from

overlying sands by Clay 2. The water levels in this well have ranged historically from 1 to 5 ft (0.30 to 1.5 m) above sea level and averaged 10 ft (3.0 m) below the base of Clay 2 during 2000, indicating that the Sand 1 aquifer is unconfined at this location. The annual water level variation in this well has been 2 ft (0.61 m) typically until the last two years when the variation has increased to 2.5 ft (0.76 m). This variation is two to three times the typical variation in the A-aquifer wells and could be due either to seasonal recharge, agricultural pumping, or both.

The vertical gradients in the FO-SVA can be derived from a comparison of the water levels in PZ-OU1-16-A, MW-OU1-11-SVA, and MW-OU1-01-180. PZ-OU1-16-A, which is screened above Clay 2, is the closest well to MW-OU1-11-SVA, which provides the only water level information from within the FO-SVA below Clay 2. Clay 2 is apparently the shallowest continuous clay layer within the FO-SVA in the OU 1 area, and therefore the change in head between the A-aquifer and the 180-foot aquifer most likely occurs within the FO-SVA below the top of Clay 2. MW-OU1-01-180 is the closest well to PZ-OU1-16-A and MW-OU1-11-SVA screened within the 180-foot aquifer.

The water level in MW-OU1-01-180 was 70 ft (21.3 m) lower than the average water level in well PZ-OU1-16-A in late 2000. This head difference equates to a downward vertical gradient of 3.6 through the FO-SVA clay layers using a total vertical clay thickness of 19.5 ft (5.9 m) between the top of the FO-SVA at PZ-OU1-16-A and the bottom of the FO-SVA at MW-OU1-01-180. The vertical gradients through the sand layers are assumed to be negligible for this calculation. The water level in MW-OU1-11-SVA was generally 60 ft (18.3 m) lower than the water level in PZ-OU1-16-A, and 10 ft (3.0 m) above the water level in MW-OU1-01-180. The head in MW-OU1-11-SVA may be representative of the head in any one of the three sand layers screened by this well within the FO-SVA. A vertical gradient of 3.5 through the clay layers below the top of Clay 2 is consistent with the head in MW-OU1-11-SVA being representative of the head in the lowermost sand screened by this well. Applying this gradient to the clay layers between the top of Clay 2 and the base of the FO-SVA, and the piezometric heads at these upper and lower boundaries, indicates that none of the sand layer aquifers in this portion of the FO-SVA are unconfined. According to this calculation, the Sand 1 aquifer has the least confinement of any of the FO-SVA aquifers, with a head at MW-OU1-11-SVA of 32 ft (9.8 m) amsl, which is ~4 ft (~1.2 m) above the base of Clay 2 at this location.

The base water level in MW-OU1-11-SVA increased by 1.5 ft (0.46 m) after storms during the early part of the 1998 hydrologic year. The water level highs increased by 2 ft (0.61 m) over the three years following the early 1998 storms and persisted through the end of 2000. The magnitude, duration, and timing of these water level shifts suggest at least a portion of the annual variation is due to seasonal recharge rather than agricultural

pumping. The difference in head between the A-aquifer and the upper sands in the FO-SVA indicates that this recharge is probably not due to a connection between the two, such as might occur if Clay 2 were absent in some areas. A possible recharge source is the Salinas River and associated alluvium, which appear to be in direct hydraulic contact with the upper sands in the FO-SVA near Blanco Road, for example.

8.6 180-Foot Aquifer Hydrology

Several wells in the vicinity of OU 1 are screened in the 180-foot aquifer as shown on Figure 8-7. The water levels in these wells have ranged from sea level to 20 ft (6 m) below sea level within the time of the water level record. Figure 8-7 also shows the fourth quarter 2000 water levels for these wells along with a piezometric surface. This quarter was chosen because it was the only one for which water level data were available for the MW-OU1-180 wells. The water levels in the MW-OU1-180 wells are 7 to 14 ft (2.1 to 4.3 m) above the base of the FO-SVA, indicating the 180-foot aquifer is confined at OU 1. The position of the base of the FO-SVA indicated by the geophysical logs from these wells was used for this calculation.

The gradient within the MW-OU1-180 well triangle is directed to the southeast, which is the opposite of the A-aquifer gradient in this area. The magnitude of the gradient is 0.00084, which is between about 1/50th and 1/5th of the A-aquifer gradient in the FDA and the vicinity surrounding the FDA, respectively. The gradient indicated by the larger pattern of 180-foot aquifer wells, namely Airfield, MW-B-05-180, and MW-B-05-180 is approximately the same. Water level records from this larger well pattern also indicate that the gradient direction does not change significantly annually, but it does increase during the dry season.

The water level records from the MW-OU1-180 wells are too short to analyze annual water level fluctuations. The water level records from MW-B-05-180 and MW-B-13-180 show an annual water level variation of 7 ft (2.1 m), while the record from the well Airfield shows an annual variation of 10 to 15 ft (3.0 to 4.6 m). The water levels in MW-B-05-180 and MW-B-13-180 increased 4 ft (1.2 m) following the early 1998 storms. The base water level increased within a year and the water level highs increased within two years. The base water level in well Airfield increased 4 ft (1.2 m) within a year while the water level high remained constant. These increases persisted through the end of 2000.

Cultivated fields are located to the east and southeast of OU 1 with largest agricultural groundwater pumping to the east-southeast. If extraction from the 180-foot aquifer for irrigation during the dry season is being done in these areas, this would explain the gradient direction, the annual shift in gradient magnitude, and the majority of the annual water level variations in this aquifer. The magnitude, duration, and timing of the water level

shift after the early 1998 storms suggest at least a portion of the annual water level variation is due to seasonal recharge rather than agricultural pumping. The 180-foot aquifer is recharged by flow from the A-aquifer at the edge of the FO-SVA, as well as by percolation of precipitation where the FO-SVA is absent.

8.7 Water Table History

Water levels near the beginning of extraction in OU 1 are available only for wells immediately surrounding OU 1. Figure 8-8 shows the 1988 water levels and corresponding contoured water table. By the second half of 1992, near steady state had been achieved in almost all of the wells based upon examination of hydrographs. Water levels and a water table from this time are shown on Figure 8-9. The gradient towards EW-OU1-17-A increases from 0.029 in 1988 to 0.037 in 1992. Figure 8-10 shows the difference between the 1988 and 1992 water tables. The water table elevations decrease around the extraction wells but maintain the same elevations in the recharge area.

Water levels and a water table from late 1997 are shown on Figure 8-11. Water levels remained fairly stable from 1992 through the beginning of 1998, rising between 1 and 2 ft (0.30 to 0.61 m) in all wells, as shown by a comparison of Figures 8-9 and 8-11. Water levels and a water table from late 2000 are shown on Figure 8-12, which uses the same well set as the previous three figures for comparison. A comparison of Figures 8-11 and 8-12 shows water levels rose significantly due to the large precipitation events in early 1998. Figure 8-13 shows the difference between these water tables. This figure indicates that the cones of depression around each extraction well decreased after the early 1998 storms. These decreases are due to the increase in transmissivity around the wells due to the water level increases combined with constant extraction rates. The changes in the cones of depression signify a decrease in the capture zone of the extraction system.

8.8 Perimeter-Well Water Table

As pre-extraction water levels are not available other than immediately adjacent to OU 1, an estimate of the regional pre-extraction water table was derived from recent post-extraction water level data as follows. Water levels perturbed by groundwater extraction and recharge as of the second quarter 2000 can be roughly determined by inspection of Figure 8-4. Eliminating the wells that have perturbed water levels and contouring the remaining water levels, located at some distance from the FDA, i.e., on the perimeter, gives a pseudo-pre-pumping water table (Figure 8-14) which we refer to as the perimeter-well water table.

The regional gradient field indicated by contouring the perimeter wells is likely representative of pre-extraction conditions. This is supported by the

regional gradients that are directed towards the western edge of the FO-SVA, where water from the A-aquifer is believed to "cascade" down to the 180-foot aquifer, and the base of the nearby bluffs overlooking the Salinas River, where several seeps are known to occur. These features are shown in brown and red, respectively (taken from Plate 3 of HLA, 1993), on Figure 8-15. Note that the perimeter-well water table gradient sweeps from northeast-trending to the east of OU 1, to northwest-trending to the west of OU 1. This understanding of the regional gradient is supported by the local gradients to the east and west of OU 1. The northeast-trending regional gradient matches the magnitude and direction of the local gradient between wells MW-B-17-A, MW-B-18-A, MW-B-19-A and MW-B-20-A almost exactly. The northwest-trending regional gradient is approximately replicated locally by the gradient between wells MW-B-10-A, MW-B-11-A and MW-B-12-A. The north by northwest trend of the regional gradient from the FDA is supported by the trend of the apparent zone of depression down gradient from the extraction wells.

Additional support for the estimated pre-extraction water table comes from evaluation of the volumetric difference between the hypothesized non-perturbed water table and the actual second quarter 2000 water table. Our analysis shows that the difference in the two water tables approximately matches expected evapotranspiration losses at the recharge area. Figure 8-16 shows the difference between these two water tables, an estimated volumetric difference of ~3 x 10^7 ft^3 (2.8 x 10^6 m^3). Using an effective porosity of 30%, this equates to a volume of water of 9 x 10^6 ft^3 (2.6 x 10^5 m^3).

Water is extracted, treated and sent through the sprinklers at the recharge area at a rate of approximately 8 gpm (5.0 x 10^{-4} m^3/s) per extraction well. This amounts to 1.3 x 10^7 ft^3 (3.8 x 10^5 m^3) over the last 12 years, although the actual amount is probably less due to extraction pump shutdowns and malfunctions. The volume of water lost during recharge consists of losses due to sprinkling inefficiency and evapotranspiration. Sprinkling efficiency is the proportion of applied water that actually enters the subsurface. A portion of the water from a sprinkler evaporates in the air and from wetted surfaces. If we use a typical value of 75% for the efficiency of a sprinkler system (e.g., Calder, 1998), about 3.2 x 10^6 ft^3 (9.1 x 10^4 m^3) of water was lost directly due to sprinkling. Taking the radius of the sprinkler area as ~100 feet (30.5 m), and evapotranspiration in the vicinity of Monterey as ~28 inches/year (71 cm/yr) (Muller and Oberlander, 1984), the total evapotranspiration loss over a period of 12 years equates to a volume of water equal to 4 x 10^5 ft^3 (1.1 x 10^4 m^3). The total estimated loss due to sprinkler inefficiency and evapotranspiration loss is 3.6 x 10^6 ft^3 (1.0 x 10^5 m^3). This compares relatively well with the water table volumetric difference of 9 x 10^6 ft^3 (2.6 x 10^5 m^3). Note that this analysis assumes that water table changes due to precipitation do not enter into the volume calculations because the water table surfaces being

differenced are from the same time. Furthermore, it is assumed that recharge of precipitation to the unconfined saturated zone is not significantly altered by the position of the water table.

8.9 Well Responses to Extraction Changes

Water levels in the two extraction wells have risen many feet for brief periods of time in the past as shown in Figure 8-17. Sometimes these changes occurred at the same time in both wells, and sometimes they occurred in only one of the wells. These changes were presumed to be due to the shutdown of the extraction pump(s). In order to determine if water levels in any surrounding wells changed in response to water level changes in the extraction wells, changes that occurred in only one of each of the extraction wells were identified as shown on Figure 8-17.

Water levels in monitoring wells surrounding the extraction wells were examined for responses to the transient water levels identified in each extraction well. The hydrographs of these wells, along with the trend lines used to determine water level responses, are shown on Figures 8-18, 8-19, 8-20, and 8-21. The well responses are mapped on Figures 8-22 and 8-23. Wells that are black on these figures could not be analyzed for response either because the well did not exist at the time, or the water level record from the well at the time of the transient could not be readily interpreted.

As shown on Figure 8-22, the response around EW-OU1-17-A is asymmetric with the wells screened above and below the Airfield Clay to the east not responding. This suggests the Airfield Clay is an important element of the hydrostratigraphic framework. As shown on Figure 8-23, the response around EW-OU1-18-A extends across at least a significant portion of the Airfield Clay. Additionally, MW-OU1-07-A responds, but MW-OU1-12-A does not respond, to changes at EW-OU1-18-A, even though these wells are about equidistant from the extraction well, are less than 100 ft (30 m) apart, and are screened in the same sand layer(s). The same lack of connectivity between MW-OU1-12-A and MW-OU1-07-A was observed during single-well pump tests as discussed in Section 9.2.

8.10 Treated Groundwater Recharge

Recharge at OU 1 occurs via two main modes: (1) treated groundwater extracted from EW-OU1-17-A and EW-OU1-18-A is sprinkled over an area to the south of the FDA; (2) precipitation in excess of evapotranspiration enters the subsurface and percolates through the unsaturated zone. In this section, we discuss the treated groundwater recharge, which amounts to approximately 0.8 in/day (2.0 cm/day) assuming a radius of 100 ft (30 m) and 8 gpm (5.0×10^{-4} m^3/s) from each extraction well, with losses as discussed in Section 8.8 that amount to approximately 30% of the sprinkled water.

The water levels in some wells decreased at the same time that water levels increased in the extraction wells as shown in Figures 8-18 and 8-19. These well responses are probably due to a decrease in the treated water recharge rate due to shutdown of one or both extraction pumps. The wells that responded are shown on Figure 8-24. Again we observe that MW-OU1-12-A responds while the nearby MW-OU1-07-A does not.

The magnitudes of the water level changes a month-and-a-half to two months after one apparent shutdown of the EW-OU1-18-A extraction pump are shown on Figures 8-18 and 8-19 and are listed in Table 8-3.

Table 8-3. Recharge area water level responses as shown on Figures 8-18 and 8-19.

Well	water level response (ft)	water level response (m)
MW-OU1-01-A	-0.79	-0.24
MW-OU1-02-A	-0.41	-0.12
MW-OU1-06-A	-0.24	-0.07
MW-OU1-12-A	-0.11	-0.03

The water level changes in Table 8-3 roughly match those measured after the shutdown of the EW-OU1-18-A extraction pump in June 2001 (see Table 9-3). The spatial distribution of the responses indicates changes in recharge affect the water table over an area approximately 500 ft (152 m) in radius centered ~150 ft (~46 m) to the south/southeast of the circle shown on Figure 8-24. The spatial distribution of the responses suggests the peak response occurs ~150 ft (~46 m) east/southeast of MW-OU1-01-A and is ~1 ft (~0.30 m). As the response is approximately conically distributed, the change in saturated volume is 6.5×10^5 ft^3 (1.85×10^3 m^3) which equates to a water volume of 2.2×10^5 ft^3 (6.2×10^3 m^3) using an effective porosity of 30%. The data in Table 9-3 also indicate that water level responses commence between 20 and 50 days after the start of the recharge change. Therefore, after a month-and-a-half to two months, the water levels have only responded to the first month of actual recharge change.

The temporal relationship between the start of the transient water level increase in EW-OU1-18-A and the water level decreases in the recharge area wells shown on Figures 8-18 and 8-19 suggests that the water level decreases began less than a month after a change in the recharge rate. The thickness of the unsaturated zone at the recharge area suggested by the water levels on Figures 8-18 and 8-19 was approximately 70 ft (21 m). Therefore the effective vertical velocity through the unsaturated zone is equal to or greater than ~3 ft/day (0.91 m/day).

The observations and conclusions above suggest that there are no laterally extensive hydrogeologic heterogeneities, such as clay layers, in the

unsaturated zone below the recharge area. First, the recharged treated water that appears to enter a relatively small area of the water table generally south of the FDA indicates no heterogeneities exist which strongly direct flow laterally. Furthermore, the rapid water level changes in response to recharge rate changes indicate the vertical flow of recharged treated water is not retarded by low permeability heterogeneities over 70 ft (21 m) of unsaturated zone.

8.11 Precipitation Recharge

The fraction of precipitation recharging the A-aquifer was determined from analysis of annual water level fluctuations in the A-aquifer wells apparently unperturbed by groundwater extraction at OU 1. These wells are shown on Figure 8-14. Of the wells shown, sufficiently long water level records are not available from MW-BW-10-A and PZ-OU1-31-A for analysis. MW-B-10-A and MW-B-14-A could not be analyzed due to the lack of a clear, annual pattern of water level fluctuations in these wells, which may indicate the presence of a hydrogeologic heterogeneity in the unsaturated zone at these locations. MW-40-01-A, MW-B-11-A, MW-B-12-A, MW-B-17-A, MW-B-18-A, MW-B-19-A, and MW-B-20-A had sufficiently long water level records exhibiting sufficient annual variation to be analyzed. Of these wells, the water level records from MW-B-17-A, MW-B-18-A, and MW-B-20-A were not analyzed due to their close proximity to MW-B-19-A, which had the highest quality water level record of the four.

The hydrograph analysis entails comparing recharge rates derived from water level changes to precipitation rates. For this analysis, water level fluctuations at each well were assumed to be due only to vertical recharge to the water table and drainage of water from the saturated zone. This obviously overlooks lateral influx of water through the saturated zone to each well. Errors due to this assumption will be discussed below.

Figure 8-25 shows schematically how the well hydrograph analysis is performed. First, the drainage rate is determined from the rate at which water levels decline during the dry portion of the year. Note that this parameter is critical and would not be possible to attain in a climate without a significant dry season. Second, the total water level increase, including both the direct increase, and the increase implied by the drainage rate, was calculated. This was performed twice for each hydrologic year: the shorter period extending from the minimum dry period water level to the maximum wet period water level, and the longer period extending from one minimum dry period water level to the next. Third, precipitation from the Monterey station was totaled over a period matching the water level change period. The start month for these totals was July for all the analysis periods, however by accounting for delays in water level increases resulting from unsaturated zone travel times, as discussed below, the length of the precipitation period used was adjusted so that the number

of rain months with significant precipitation matched the number of months in the associated water level period in all but a few cases. Finally, the total water level increase and the total precipitation for each period were divided by the number of days in the period. The resulting values for all the periods for all the wells analyzed are shown on Figure 8-26, from which recharge rates can be measured. However, the differences between the water level responses for each well provide an understanding of the magnitude of the error introduced by neglecting the lateral influx of water through the saturated zone to each well in the recharge analysis.

Figure 8-26 indicates the closer a well is to the edge of the FO-SVA, the greater the water level changes in response to precipitation. For instance, the changes in MW-B-11-A, which is close to the edge of the FO-SVA, are approximately twice that at MW-B-19-A, which is far from the edge of the FO-SVA. As the groundwater flow through the saturated zone increases toward the edge of the FO-SVA, the variation in well response is presumably an indication of the error introduced by ignoring lateral flow to the well through the saturated zone. The implication of this understanding is that the lower water level response trends should be used for the recharge calculations in order to minimize the error associated with neglecting lateral groundwater flow.

The Monterey station average precipitation rate for the period 1989–2000 adjusted to the Fritzsche AAF station value is 0.047 in/day (0.12 cm/day) (adjustment discussed in Section 8.2). From Figure 8-26, this daily average precipitation rate correlates to a daily water level increase of 0.0035 ft/day, or 0.042 inches/day (0.11 cm/day). This daily water level increase is on the low side of the water level response scatter in order to reduce the impact of lateral groundwater flow as discussed above. Using an effective porosity of 30% for the sandy capillary fringe region of the A-aquifer, this equates to a recharge of 0.013 in/day (0.033 cm/day). Dividing the daily recharge rate by the daily average precipitation at Fritzsche AAF suggests that approximately 27% of the average precipitation percolates to the water table.

Various complications were encountered during the analysis described above. First, the apparent drainage rate in all wells varied from dry season to dry season. These differences were probably due to variations in the temporal pattern of precipitation from year to year. This was resolved by using the maximum drainage rate, or an average of several maximum rates, in the analysis. Second, the drainage rate differed in some wells depending upon dry season water level. When significantly different drainage rates appeared to be present, the higher water levels correlated to a greater drainage rate, presumably due to increased transmissivity. In these instances, the drainage rate appropriate to a particular base year water level was used. Third, the timing of the maximum water levels in several wells occurred months after the maximum monthly precipitation. The size of this delay was determined by looking at the timing of all the

water level peaks relative to the monthly precipitation maximums. This delay was used to correct the number of months over which precipitation was totaled for the short (sub-year) recharge periods. Finally, the 1998 and 1999 hydrologic year results frequently appeared low and high, respectively, probably due to continued drainage of the 1998 precipitation from the unsaturated zone into the saturated zone in 1999. No attempt was made to correct this error.

As shown on Figure 8-2, total precipitation during the 1998 hydrologic year was significantly greater than during any other hydrologic year during which water level data from the site were available. Figure 8-27 shows the monthly precipitation totals during the 1998 hydrologic year. The most significant aspect of this hydrologic year was the large of amount of rainfall in both January and February. The water levels in all the A- aquifer wells in the study area started rising within three months of the January/February 1998 storms. The timing of these water level increases was interpolated from each well's hydrograph, as shown on Figure 8-28. The results of this interpolation are shown for each well on Table 8-4.

Table 8-4. Timing of water level increases after early 1998 storms.

well	Approximate month in which water level increase began	well	Approximate month in which water level increase began
MW-B-10-A	April	MW-OU1-05-A	April/May
MW-B-11-A	March	MW-OU1-06-A	April
MW-B-12-A	February	MW-OU1-07-A	April
MW-B-14-A	April	MW-OU1-08-A	April
MW-B-17-A	March	MW-OU1-09-A	May
MW-B-18-A	March	MW-OU1-10-A	May
MW-B-19-A	February	MW-OU1-12-A	March
MW-B-20-A	February	MW-OU1-19-A	May
EW-OU1-17-A	May	MW-OU1-20-A	April/May
EW-OU1-18-A	April	MW-OU1-21-A	March/April
MW-40-01-A	February	MW-OU1-22-A	May
MW-OU1-01-A	April	MW-OU1-23-A	May
MW-OU1-02-A	April	PZ-OU1-13-A	April
MW-OU1-03-A	April	PZ-OU1-14-A	May
MW-OU1-04-A	May	PZ-OU1-15-A	April
		PZ-OU1-16-A	April

Figure 8-29 shows the relationship between the unsaturated zone thickness at each well and the amount of time between the end of January 1998 and the beginning of the water table rise. Figure 8-29 suggests that the January/February 1998 precipitation signal traveled to a depth of 60 ft (18.3 m) below ground surface (bgs) in less than a month. This is perhaps

due to wetting of this interval by precipitation events earlier in the year. This hypothesis is supported by water level response times of less than one month to changes in the rate of recharge as discussed in Section 8.11.

At depths greater than 60 ft (18.3 m) bgs, the timing of the water level increase is proportional to the thickness of the unsaturated zone in excess of 60 ft (18.3 m). This indicates an average vertical flow velocity of 20 ft/month, or 0.7 ft/day (0.21 m/day), in this deep portion of the unsaturated zone. The proportionality also suggests that the water level rise at each well was due at least initially to vertical recharge in the vicinity of the well, rather than influx of water laterally through the saturated zone, and that there are no laterally extensive hydrogeologic heterogeneities, such as clay layers, in the unsaturated zone. This is in accord with the conclusions regarding the unsaturated zone hydrogeology in Section 8.10.

8.12 Contaminant Distribution

Figure 8-30 lists all the organic compounds consistently detected in groundwater at each well, where the word "detection" indicates concentrations above the PQL. Consistent detection in a well is loosely defined as a compound detected in all samples over the course of a year, or detected in half of all samples taken from the well. Thus many compounds are listed on the map which were detected consistently early in a well's history, but which have since dropped below the detection limit.

The A-aquifer at OU 1 contains contaminated groundwater. The Sand 2/3 aquifer beneath the Airfield Clay also contains contaminated groundwater as indicated by results from MW-OU1-33-A. The groundwater in the shallow aquifers in the FO-SVA are uncontaminated as indicated by results from MW-OU1-11-SVA. Groundwater in the 180-foot aquifer is not contaminated based upon results from one quarter of sampling from the recently installed 180-foot aquifer wells in and near the Fire Drill Area.

Figure 8-30 shows the extent in the A-aquifer of the most widely detected organic compounds. These compounds are the chlorinated volatile organic hydrocarbons (VOCs) trichlorethylene (TCE), 1,2-dichlorethylene (DCE), 1,1,1-trichlorethane (TCA), and 1,1-dichlorethane (DCA). The plumes shown are not for a particular time, but rather include wells where a particular compound was consistently detected at any time.

8.13 TCE Distribution and Concentration Trends

As already recognized, TCE is the most widely distributed VOC, and occurs at the highest concentrations in groundwater at OU 1 (HLA, 1998a). Figure 8-31 shows the TCE concentration history overlaid on the hydrograph for each well. The changes in the TCE concentration at each well are summarized on Table 8-5. Wells with insufficient data to analyze TCE concentration trends, such as MW-B-11-A, are not included in the

table. MW-OU1-A wells beyond number 20 are not included in the table due to a combination of the one or more of the following: all concentration results ND, concentrations erratic, or concentration record too short to interpret. MW-OU1-21-A and MW-OU1-23-A are exceptions as their concentration records can be interpreted despite their short durations.

Table 8-5. Summary of TCE concentration changes.

well	pre-1998 TCE concentration change	post-1997 TCE concentration change	post-1998 change occurs by quarter	start of 1998 water level rise	water level rise two quarters after start (ft)	water level rise four quarters after start (ft)	maximum water level rise by the end of 2000 (ft)
MW-OU1-01-A	decreasing	none		April, 1998	2.13	4.28	6.20
MW-OU1-02-A	Indiscernible due to all ND	increase	1999, but only with one sample result, and exact timing indiscernible due to annual sampling and ND baseline	April, 1998	2.46	4.18	6.30
MW-OU1-03-A	decreasing	none		April, 1998	2.59		6.74
MW-OU1-04-A	increasing (from ND or projected ND in 1988)	increase	Q3, 1998	May, 1998	2.92	6.93	10.42
MW-OU1-05-A	increasing	increase	Q3, 1998	April/May, 1998	2.82	6.54	11.86
MW-OU1-06-A	decreasing	increase	Q2, 1998	April, 1998	2.29	4.41	6.79
MW-OU1-07-A	decreasing	none		April, 1998	2.30	4.07	6.53
MW-OU1-08-A	decreasing	increase	timing indiscernible due to gradual increase	April, 1998	2.63	4.14	6.88
MW-OU1-09-A	indiscernible due to all ND	Indiscernible due to all ND		May, 1998	2.55	6.11	9.93
MW-OU1-10-A	indiscernible due to all ND	increase	Q1, 1999, but exact timing indiscernible due ND baseline	May, 1998	2.57	6.32	10.12
MW-OU1-11-SVA	indiscernible due to all ND	indiscernible due to all ND		mid-1998			
MW-OU1-12-A	decreasing	none		March, 1998	1.43	3.41	6.65
EW-OU1-17-A	decreasing slightly	increase	Q2, 1998 possibly, but Q2, 1999 certainly	May, 1998	5.97	9.72	18.3
EW-OU1-18-A	decreasing	none		April, 1998	2.55		6.73
MW-OU1-19-A	increasing from ND in 1988	increase	Q3, 1998	May, 1998	2.74	6.37	10.27

MW-OU1-20-A	none	increase	Q1, 1999	April/May, 1998	2.26	4.10	7.21
MW-OU1-21-A	insufficient data	increase	Q2, 1999, but exact timing indiscernible due ND baseline	March/April, 1998	2.13	4.13	8.15
MW-OU1-23-A	insufficient data	increase	Q3, 1998 possibly, but Q1, 1999 certainly	May, 1998	2.63	5.94	10.58
MW-40-01-A	indiscernible due to all ND	increase	timing indiscernible due ND baseline	February, 1998	3.36	3.88	6.51
MW-B-10-A	indiscernible due to all ND	indiscernible due to all ND		April, 1998	3.49	5.35	6.55
MW-B-14-A	indiscernible due to all ND	increase	timing indiscernible due ND baseline	April, 1998	3.46	5.18	6.01
MW-B-17-A	indiscernible due to all ND	indiscernible due to all ND		March, 1998	2.03	3.62	4.64

The TCE plume in late 1993, early 1994 is shown on Figure 8-32. At this time, which is more than five years after the start of extraction, treatment and recharge, the plume occupies the FDA and area to the west and northwest. The northern extent of the plume is unknown. The trends shown on Figure 8-31 indicate the TCE concentrations in MW-OU1-04-A, MW-OU1-05-A, and MW-OU1-19-A to the northwest of the FDA increased from an initial or projected initial value of ND, which suggests that the plume did not occupy the area west and northwest of the FDA at the start of the pump-and-treat operation.

The TCE plume in late 1997 is shown on Figure 8-33. The pre-1998 TCE trend at each well, as listed on Table 8-5, is also indicated. At this time, the plume had shifted to the west and northwest of the FDA. The northern extent of the plume is still unknown.

The TCE plume in late 1999 is shown on Figures 8-34 and 8-35. The post-1997 TCE trend at each well, as listed on Table 8-5, is also indicated. The plume has not shifted significantly since late 1997, shown on Figure 8-33. Rather the concentrations have increased further in the pre-existing plume area to the west and northwest of the FDA. The northern extent of the plume is still unknown, although it was known to extend far to the north of the FDA in 1999, as shown on Figure 8-35. The position of the northern part of the plume in 1999 appears to be downgradient of the FDA, as shown on Figure 8-14. Furthermore, the average gradient from the FDA to the northern end of the plume is 0.007. Using an average hydraulic conductivity of 1.8×10^{-5} m/s (5.1 ft/day) (see Section 9.2), we obtain a Darcy velocity of 0.036 ft/day (0.0109 m/day). Assuming an average porosity of 30%, the average pore velocity is 0.12 ft/day (0.036 m/day). Multiplying this average velocity by 39 years (the time since start of fire fighter training at the FDA) gives a length of 1680 ft (510 m), which matches the actual plume length to within a factor of two. These results suggest that no additional contaminant sources, hydrogeological heterogeneities, or anisotropies are required to explain the position of the plume to the north.

The location of the TCE decreases shown on Figures 8-33 and 8-34 suggests they resulted from migration of treated groundwater from the recharge area to EW-OU1-18-A. The pre-1998 and post-1997 TCE increases to the west and northwest of the FDA could have occurred because of gradient changes. Alternatively, the increases could have occurred due to mixing of pore waters with relatively higher TCE concentrations at the base of the unsaturated zone into the groundwater as a result of rising water levels, or because flow from the recharge area down to the water table passed through a zone of TCE-contamination in the unsaturated zone to the west and northwest of the FDA. These different hypotheses, and the likelihood of each, are summarized on Table 8-6. An explanation for the likelihood of each hypothesis follows.

Table 8-6. Hypotheses and likelihoods for TCE increases.

timing of TCE increase W/NW of Fire Drill Area	gradient change	water level increase	recharge through TCE-contaminated unsaturated zone
pre-1998	possible	unlikely	possible
post-1997	unlikely	unlikely	possible

In the years following the commencement of the GTS, the gradient along the west edge of the FDA shifted from north-directed to northwest-directed due to mounding of water beneath the recharge area, as indicated by a comparison of Figures 8-14 and 8-9. The timing of this change suggests gradient changes could be responsible for the pre-1998 TCE increases west and northwest of the FDA. A comparison of Figures 8-11 and 8-12 indicates there was no significant change in the gradient direction in the FDA after 1997, despite the rise in the water table, suggesting gradient changes could not be responsible for the post-1997 TCE increases.

The water levels west and northwest of the FDA generally decreased from 1988 to 1993, as shown on Figure 8-10, and then rose slightly (1 to 2 ft (0.30 to 0.61 m)) through early 1998. Therefore water level increases cannot explain the pre-1998 TCE increases in this area. The water table did rise significantly following the early 1998 storms, however the timing of the post-1998 TCE concentration increases does not correlate to the timing or the rate of the water table rise as shown in Table 8-5.

The timing of well-constrained post-1998 TCE concentration increases is shown on Figure 8-36. This pattern is consistent with TCE entering the saturated zone west of the FDA nearer to MW-OU1-06-A and then flowing north toward EW-OU1-17-A. The lack of water level rise prior to 1998 suggests that the TCE was transported to the water table by recharge water that was contaminated during its passage through the vadose zone. This is supported by the lack of 1,2-DCE and 1,1-DCA, degradation products of TCE and 1,1,1-TCA, respectively, as shown on Figure 8-30, which indicates this portion of the groundwater plume is younger than the rest of the plume. The appearance of contaminated groundwater to the west and northwest of the FDA after commencement of recharge, and the concentration increases after the 1998 recharge event, suggest that the zone of TCE-contaminated pore water in the vadose zone is located near a hydrogeologic heterogeneity where only large flows can pass through it, such as beneath a clay layer.

Figure 8-36 and Table 8-5 show that the last post-1998 TCE concentration increase starts in early 1999 in wells MW-OU1-20-A, screened above the Airfield Clay, and possibly MW-OU1-23-A, screened just downgradient of the edge of the Airfield Clay. The timing of these increases, along with the relatively low TCE concentration in MW-OU1-08-A and the relatively high concentration in MW-OU1-39-A, suggests they could be due to contaminated groundwater flowing from the area west and northwest of the FDA between the two extraction wells and into the saturated zone above the Airfield Clay. The change in the shape of

the capture zones following the early 1998 storms, as discussed in Section 8.7, may have allowed some groundwater flow between the two extraction wells. Alternatively, a significant heterogeneity could allow groundwater to flow between the two extraction wells. The water table gradients shown on Figure 8-4 make either explanation seem rather unlikely, however, as they suggest flow would have to be occurring almost perpendicular to the gradient. The flow vector measured in MW-OU1-39-A shown in Table 9-4 matches the gradient direction fairly well.

A more likely alternative hypothesis to explain the post-1998 TCE concentration increases above the Airfield Clay is the existence of a source of TCE, or residual unsaturated zone contamination, east of the FDA. This source has to be sufficiently far upgradient that the TCE increases on top of the Airfield Clay at MW-OU1-20-A occur a year after the early 1998 storms. The lack of a TCE increase at MW-OU1-03-A and the pattern of TCE concentrations in wells above the Airfield Clay suggest that the source must be downgradient of MW-OU1-03-A, but closer to MW-OU1-39-A than to MW-OU1-08-A. The most likely position of the source under this hypothesis is approximately 50 ft (15.2 m) north/northwest of MW-OU1-03-A.

We emphasize that this additional potential source of TCE is suggested to explain local TCE concentration changes above the Airfield Clay, and is not required to explain the overall TCE plume geometry.

8.14 Natural Attenuation

Sufficient data on cation and anion concentrations are not available to assess the redox potential of the groundwater at OU 1. However, Figure 8-30 shows the presence of 1,2-DCE and 1,1-DCA, which are degradation products of TCE and 1,1,1-TCA, respectively, indicating reductive dechlorination is occurring at OU 1. Reductive dechlorination in the groundwater at OU 1 appears to be slight and relatively unimportant in limiting the extent of the plume, however, for reasons as follows. The 1,2-DCE and 1,1-DCA plumes are entirely within the TCE and 1,1,1-TCA plumes, respectively, as shown on Figure 8-30. Generally, if reductive dechlorination is limiting a plumes extent, the degradation product plumes are located downgradient of the parent product plume. Figures 8-37 and 8-38 show that the distribution of TCE to 1,2–DCE, and 1,1,1-TCA to 1,2–DCA concentration ratios, respectively, are low and do not increase downgradient, both of which are contrary to the presence of significant reductive dechlorination. As a result, the extent of groundwater contamination is probably controlled primarily by dilution and retardation.

9.0 FLOW SENSOR EVALUATION

9.1 Introduction

The Hydrotechnics ISPFS was developed at Sandia National Laboratory and commercialized by Hydrotechnics as a method of estimating the groundwater flow (Darcy) velocity, i.e., both magnitude and 3D flow direction (Ballard, 1996a), which can be converted to pore velocity by dividing by porosity. The flow sensor consists of a uniformly heated cylinder 2.5 ft (0.76 m) in length by 2 in (0.05 m) in diameter that is installed in a borehole while allowing the formation to collapse around the instrument, or alternatively by backfilling the annulus around the instrument with native soils. An array of thirty temperature sensors located on the surface of the cylinder monitors the temperature field in the surrounding water-saturated formation. Groundwater flow through the formation and past the instrument distorts the thermal field around the heater, resulting in relatively cool temperatures being measured on the upstream side of the sensor, with relatively warm temperatures on the downstream side. Based on the distortion of the thermal field both components of the groundwater flow (magnitude and direction) can be determined during the data processing step. The software that processes the measured temperature data assumes the formation is thermally homogeneous and of infinite extent.

Hydrotechnics flow sensors were co-located at OU 1 with dedicated low-flow groundwater sampling pumps in the five wells installed in this project (MW-OU1-36-A, MW-OU1-37-A, MW-OU1-38-A, MW-OU1-39-A, and MW-OU1-40-A). Table 9-1 shows the distance between the bottom of each flow sensor and the top of the first clay layer encountered. The flow sensor co-located with MW-OU1-40-A experienced an electrical short downhole in January 2001 and the heater failed. Therefore, no flow data were available from that sensor, although the thermistors continued to provide information on the unperturbed thermal field in the A-aquifer.

We conducted pump tests in the A-aquifer at OU 1 that served to perturb the flow field and thereby test the ISPFS response. Below we present results of pump test analysis and ISPFS response, with emphasis on comparing ISPFS measurements to traditional methods of analysis.

Table 9-1. Location of the ISPFSs in relation to the top of the first clay layer encountered.

Location	Elevation above mean sea level							
	Top of sensor		Bottom of sensor		Top of first clay encountered		Distance from sensor to clay	
	ft	m	ft	m	ft	m	ft	m
MW-OU1-36-A	42.4	12.9	39.9	12.2	35.9	10.9	4.0	1.2
MW-OU1-37-A	38.8	11.8	36.3	11.1	35.8	10.9	0.5	0.15
MW-OU1-38-A	40.9	12.5	38.4	11.7	37.4	11.4	1.0	0.30
MW-OU1-39-A	51.4	15.7	48.9	14.9	47.4	14.4	1.5	0.46
MW-OU1-40-A	37.4	11.4	34.9	10.6	25.9	7.9	9.0	2.7

9.2 Short-Duration Pump Tests

We conducted short-duration pump (extraction) tests from May 7 to May 10, 2001 in wells located at OU 1. The primary objective of the testing was to explore the feasibility of short-duration cross-hole pump tests to investigate formation anisotropy and to perturb the flow field on a scale sufficient to test the ISPFSs. The secondary objective was to provide estimates for the local formation hydraulic conductivity. The parameters determined from the analysis of extraction test data can be used to constrain hydrological models of the A-aquifer. The Dupuit-Forchheimer equation, an analytical solution used to model radial flow in an unconfined aquifer, was used to estimate the hydraulic conductivity. Based on the acquired data set, the hydraulic conductivity was observed to vary between 3.6 ft/day (1.1×10^{-5} m/s) to 42 ft/day (1.5×10^{-4} m/s), corresponding to permeabilities of approximately 1.2×10^{-12} m^2 to 1.6×10^{-11} m^2.

Tests were conducted by installing a pump and pressure transducer in an extraction well, with nearby observation wells instrumented with pressure transducers to monitor crosshole water level changes. The pressure transducers are sensitive to water level changes as small as three millimeters. Table 9-2 lists the tests performed and the observation wells that were monitored. The only test conducted that had a discernable crosshole response was the test in borehole MW-OU1-29-A, which showed changes in observation borehole PZ-OU1-35-A, located 30 ft (9.1 m) from the extraction well. These wells are located in the northern part of OU 1 where the permeability is very large (see Table 9-2).

Table 9-2. Short-duration pump test results.

Pumped Well	Observation well(s)	Crosshole response, distance to observation well, ft	m	Volume extracted, gal	m^3	Hydraulic conductivity, m/s
		No				
MW-OU1-08-A	MW-OU1-32-A MW-OU1-33-A	217 217	66.1 66.1	105	0.40	1.1×10^{-5}
		No				
MW-OU1-07-A	MW-OU1-12-A MW-OU1-36-A MW-OU1-37-A	86 156 129	26.2 47.5 39.3	1010	3.82	1.2×10^{-5}
		Yes				
MW-OU1-29-A	PZ-OU1-35-A	30	9.1	100	0.38	1.5×10^{-4}
		No				
MW-OU1-10-A	MW-OU1-9-A MW-OU1-19-A	153 189	46.6 57.6	100	0.38	2.5×10^{-5}
		No				
MW-OU1-6-A	MW-OU1-36-A	166	50.6	100	0.38	N/A

The volume of water extracted during each test was approximately 100 gal (0.38 m^3). The general volume limitation was based on the size of the truck-mounted storage tank that was used to transport produced water to the OU 1 granular activated carbon treatment system. For the MW-OU1-7-A test, the pump outlet was connected directly into the OU 1 treatment system, and a total of 1010 gal (3.8 m^3) were extracted.

Data from all wells tested are presented in Figures 9-1 to 9-5. Figure 9-5 shows the data from the only test with a measurable crosshole response. Note that the hydraulic head in MW-OU1-29-A (Figure 9-5) does not recover to the pre-pumping level due to complications in field testing caused by a chemical-sampling device that was located in the extraction borehole. An effort was made to minimize the time the sampling device was not in the wellbore. As soon as the pump was lowered to the bottom of MW-OU1-29-A the pump was turned on. The measured water level reflects the upward displacement of the free-surface within the well caused by lowering the pump into the well. The actual drawdown

is assumed to be the difference between the water level during pumping and the recovered level after pumping was stopped.

The Dupuit-Forchheimer equation used to process the data assumes an outer boundary radius R and wellbore radius r along with the measured steady-state drawdown h and flowrate Q, to estimate the saturated-hydraulic conductivity K as:

$$K = \left(\frac{Q}{\pi\left(h^2 - H^2\right)} \right) \ln\left(\frac{r}{R}\right) \qquad (9\text{-}1)$$

where h is the elevation of the free surface in the wellbore and H is the elevation of the piezometric surface at radius R. Using Equation 9-1, the hydraulic conductivity was estimated based upon an assumed outer boundary radius of 66 ft (20 m) and an effective wellbore radius of 0.5 ft (0.15 m) (Table 9-2). The MW-OU1-6-A test has not been analyzed because the drawdown was still increasing rapidly when the pumping portion of the test was terminated. Since the true piezometric profile is above the free surface measured in the wellbore in all wells, the Dupuit-Forchheimer equation will tend to underestimate the formation hydraulic conductivity.

9.3 Shut-down of EW-OU1-18-A

To induce flow changes that could be detected by the ISPFSs as well as creating cross-hole response, we conducted a large-scale test that took advantage of the approved shutdown of pumping well EW-OU1-18-A by Harding ESE. Since relatively steady extraction had been ongoing for 12 years, the shutdown of EW-OU1-18-A provided a significant perturbation to the flow system that could be used to look at larger scale properties of the A-aquifer than could be investigated using the single-well extraction tests. Two different monitoring methods were used: (1) traditional hand measured depth-to-water (DTW) and electronic pressure transducer measurements of piezometric head; and (2) the new network of ISPFSs to measure changes in the Darcy velocity of the groundwater. Analyses by these two approaches are presented below.

9.4 Analysis of Piezometric Data

The EW-OU1-18-A pump was shut down on June 20, 2001 at 11:30 AM with measurements of water levels made just prior to pump shutdown and again on June 21, July 10, and August 12, 2001. A list of the wells that were monitored and the DTW measurements that were obtained is shown in Table 9-3. The last column of Table 9-3 shows the overall change in DTW as calculated using the August 12, 2001 DTW subtracted from the average pre-test DTW.

Table 9-3. Depth to water and net change before and after shutdown (ft).

Well Number	Prior to Pump Shutdown			Post Pump Shutdown			Net Change
	6/18/01	6/19/01	6/20/01	6/21/01	7/10/01	8/12/01	
MW-OU1-01-A	71.93			71.98	72.3	72.55	-0.62
MW-OU1-03-A	77.68	77.66		77.34	76.84	76.89	0.78
MW-OU1-04-A		90.05		89.98	89.66	89.5	0.55
MW-OU1-05-A		88.4		88.42	88.28	88.33	0.07
MW-OU1-06-A	75.58			75.62	75.64	75.8	-0.22
MW-OU1-07-A		63.23		63.2	62.94	63.05	0.18
MW-OU1-08-A	91.65	91.68		91.68	91.48	91.45	0.215
MW-OU1-09-A			84.1	84.14	84.02	84.08	0.02
MW-OU1-10-A			86.92	87.02	86.84	86.84	0.08
MW-OU1-12-A	63.14			63.16	63.22	63.38	-0.24
PZ-OU1-14-A	94.52			94.58	94.32	94.2	0.32
PZ-OU1-15-A			73.16	72.38	71.78	71.86	1.3
MW-OU1-16-A			73.64	72.96	72.44	72.5	1.14
EW-OU1-17-A				96.2	95.86	95.61	
EW-OU1-18-A	76.78			72.52	71.94	72.03	4.75
MW-OU1-19-A		91.56		91.62	91.48	91.58	-0.02
MW-OU1-20-A		99.06		99.06	98.94	98.87	0.19
MW-OU1-23-A	99.04			99.16	99.04	99.05	-0.01
MW-OU1-25-A			97.52	97.6	97.48	97.54	-0.02
MW-OU1-32-A	84.04	83.98		84.06	83.96	83.98	0.03
MW-OU1-33-A	88.6	88.62		88.66	88.56	88.57	0.04
MW-OU1-36-A		61.94		62	62.02	62.16	-0.22
MW-OU1-37-A		63.28		63.22	63.1	63.26	0.02
MW-OU1-38-A		80.95		80.96	80.82	80.94	0.01
MW-OU1-40-A		91.4		91.84	91.78	91.68	-0.28
MW-BW-10-A	74.48			74.52	74.62	74.84	-0.36

Pressure transducer measurements were performed using a combination of submersible transducers manufactured by Druck Inc. and Pressure Systems Inc. with wiring connected to the shipping container in the FDA using temporary cables that traversed the ground surface. A Fluke Hydra scanning data logger was used to measure the voltage output from all sensors and to store them on a personal computer. The data showed unexpected and large amounts of noise that varied significantly from location to location. In particular, there was a large diurnal DC offset that may have been caused by electrical equipment cycling on and off at the nearby Marina Airport. Because the changes in the water levels from the pressure transducers could not be reconciled with the hand DTW measurements, the electronic data are not presented here. For the short term extraction tests conducted using similar pressure transducers and monitoring equipment, it should be noted that the cable runs were significantly shorter, and the data did not show any of the noise that was present during the long term monitoring.

The August 12, 2001 DTW measurements are used as a reference for changes in the piezometric surface caused by the shutdown of EW-OU1-18-A. The responses of the monitored wells to the shutdown of EW-OU1-18-A can be separated into three basic types: (1) increases in the piezometric head, (2) no significant change (less than 0.1 ft (.03 m) change) and (3) decreases in the piezometric head. When the responses were categorized this way they fell into

distinct spatial groups. The wells located around the recharge area in the FDA showed a decrease in the piezometric head. The wells that showed an increase in the piezometric head were all located near the pump well or slightly to the north. Wells that showed no change were located west and east of EW-OU1-18A or far to the north.

Well MW-OU1-01-A, which is located approximately 150 ft (45.7 m) southwest of the recharge area showed the largest decrease in head, 0.61 ft (0.19 m). About 200 ft (61 m) farther to the south is MW-BW-10-A, which showed a significant but smaller decrease of 0.36 ft (0.11 m). Wells MW-OU1-06-A, MW-OU1-12-A, and MW-OU1-36-A located south of EW-OU1-18-A but north and west of the recharge area all showed decreases of about 0.22 ft (0.067 m). These decreases are caused by the lower rate of recharge from the sprinkler due to the turning off of EW-OU1-18-A and the associated shrinking of the groundwater mound.

Using the August 12, 2001 DTW measurements as a baseline, the pumped well, EW-OU1-18-A, shows a recovery of 4.75 ft (1.4 m). Nearby piezometers PZ-OU1-15-A and MW-OU1-16-A, located 14.3 ft (4.4 m) and 27.6 ft (8.4 m) from the pumped well, showed increases of head of 1.3 ft (0.40 m) and 1.1 ft (0.33 m), respectively. MW-OU1-03-A, located 53 ft (16 m) northeast of the pumped well and MW-OU1-04-A located 332 ft (101 m) northwest of the pumped well showed increases in head of 0.78 ft (0.24 m) and 0.55 ft (0.17 m), respectively. MW-OU1-07-A, which is 210 ft (64 m) southwest of the pumped well showed an increase of only 0.18 ft (0.055 m). This small increase can be attributed to the location of the well between the extraction well and the mounded recharge area. Similarly, MW-OU1-37-A, located 178 ft (54 m) south of the extraction well showed virtually no change in head (0.02 ft (0.006 m). Wells PZ-OU1-14-A, MW-OU1-20-A, and MW-OU1-08-A located north of EW-OU1-18-A at distances of 350 to 450 ft (107 to 137 m), showed increases of approximately 0.2 ft (0.061 m).

9.5 Responses of the ISPFSs

Figures 9-6 through 9-9 show output from Hydrotechnics data processing application HTFlow95 (version 2.00) consisting of estimated horizontal Darcy groundwater flow magnitudes and azimuths for the four working flow sensors from February 18, 2001 until August 17, 2001. Large changes in estimated velocities caused by the shutdown of EW-OU1-18-A on June 20, 2001 are observed in the flow sensor data for MW-OU1-36-A, MW-OU1-37-A and MW-OU1-38-A. The flow sensor in MW-OU1-39-A experienced a decrease in the power being supplied to the heater on June 5, 2001 causing a perturbation in the estimated velocity field that swamped any potential changes caused by turning off the extraction well pump. As shown in the figures, three of the ISPFSs show rapid responses to the change in flow field induced by the pump shutdown on June 20, 2001.

The actual measurements used to estimate velocities are the temperatures along the surface of the sensor. Figures 9-10 through 9-13 show the measured

temperature fields before and after the shutdown of EW-OU1-18-A. For both MW-OU1-36-A (Figure 9-10) and MW-OU1-37-A (Figure 9-11), large changes in the temperature time history are evident starting on the day the pump was shut off. MW-OU1-38-A (Figure 9-12) showed more subtle changes in temperatures that are interpreted by the HTFlow95 software as representing a change in vertical flow velocity but not horizontal velocity. In MW-OU1-39-A the shutdown of EW-OU1-18-A produced no clear effect on the sensor temperature profile and, because of the aforementioned change in power to the flow sensor heater, the results could not be interpreted.

The magnitudes of the vertical velocities are striking in that they are larger than the horizontal velocities and they are directed downward toward the underlying low-permeability clay. Previous users of the Hydrotechnics flow sensor have also noted anomalously high apparent downward flow (Ballard, 1995; Ballard et al., 1996). As discussed by Ballard (1995), a possible explanation for the apparent large downward velocities is that HTFlow95 calculates velocity assuming that the surrounding formation is homogeneous in its thermal properties, whereas the natural system is known to be layered. Clay has a lower thermal conductivity than the overlying A-aquifer sands. Since the flow sensors were installed just above the clay, the temperature field can be distorted by the lower thermal conductivity of water-saturated clay relative to water-saturated sands, thereby increasing the temperature at the base of the flow sensors. If the temperatures are greater near the bottom of the probe than at the top, the HTFlow95 interprets the skewed temperature field as being caused by downward flow, even if the actual cause is thermal conductivity variation.

We compared the temperature field in MW-OU1-36-A with that in MW-OU1-40-A, the sensor no longer being heated. Figure 9-14 shows a plot of temperature for MW-OU1-36-A as a function of the length (L) along the probe. The top of the flow sensor is approximately two degrees cooler than the bottom of the sensor. To show that this temperature gradient does not exist naturally in the A-aquifer, the same temperature profile taken August 13, 2001, was examined in the flow sensor at MW-OU1-40-A. The natural temperature field in MW-OU1-40-A is 0.08°C cooler on the bottom of the flow sensor than on the top, as seen in Figure 9-15. We conclude from this comparison that the asymmetry of the thermal anomaly created by the heated ISPFS is not related to natural temperature gradients, but rather appears to be caused by heterogeneity in thermal properties associated with the layered sediments. Further investigation of the cause of the apparent downward flow should be carried out since actual downward flow, if present, could lead to the contamination of the underlying aquifer. Future work should exploit the non-isothermal simulation capabilities of TOUGH2 (Pruess et al., 1999) to investigate the origins of apparent vertical velocities around ISPFSs, and importantly, provide additional information on likely actual vertical velocity components.

The horizontal velocities as estimated by the flow sensors in MW-OU1-36-A and MW-OU1-37-A both decreased after the EW-OU1-18-A pump shutdown. MW-OU1-38-A showed no appreciable change in horizontal velocity. A simple flow

model was developed to compare against the ISPFS horizontal velocity measurements. The simple flow model uses a combination of Darcy's Law and steady-state fluxes associated with the two extraction wells and the recharge area. Because of natural permeability variations and changes in the thickness of the saturated zone above the FO-SVA, a one-to-one correspondence between ISPFS results and the simple model predictions should not be expected. Nevertheless, the flow sensor data should provide a reasonable overall picture of hydraulic behavior. The model assumes that Darcy's Law can be applied to calculate a net groundwater flow based on the overall piezometric gradient for the OU 1 region. Darcy's Law relies upon measurements of piezometric head, h, at monitoring well locations to estimate the fluid Darcy velocity

$$v_s = -K\frac{\partial h}{\partial s} \tag{9-2}$$

where s is the direction of maximum head gradient. Neglecting the local disturbances in the piezometric surface due to pumping at EW-OU1-17-A, EW-OU1-18-A and the treated water recharge area, the hydraulic gradient was assumed to be 0.012 (see Section 8.4) and to have an azimuth of 330°. The hydraulic conductivity was assumed to be 1.8×10^{-5} m/s (5.1 ft/day), which represents the harmonic mean obtained from the short-duration pump tests (Section 9.2).

Darcy's Law provides an estimated background velocity without the influences of pumping and recharge of 2.15×10^{-7} m/s (0.061 ft/day). To account for the influences of pumping and recharge, Darcy velocities can be calculated assuming superposition of uniform cylindrical flow fields at each pumping and recharge location. Figure 9-16 shows a streamline map of the flow field assuming the net background velocity is combined with the effects of pumping at EW-OU1-17-A and EW-OU1-18-A at 8 gpm (5.0×10^{-4} m^3/s) and 80% of the extracted volume is recharged at the south end of the FDA. Figure 9-17 shows a similar streamline map with the exception that EW-OU1-18-A was assumed to be turned off.

Table 9-4 shows a comparison of flow sensor and simple flow model estimates for horizontal Darcy velocity and flow direction for MW-OU1-36-A, MW-OU1-37-A, and MW-OU1-38-A. The differences in velocities estimated by the flow sensors and by the model are within the range of natural variability and uncertainty of the permeability field. The measurements made at MW-OU1-36-A and MW-OU1-37-A also show good agreement in groundwater flow direction. The MW-OU1-38-A flow direction is not consistent with the simple model, and may indicate either a mistake in the alignment of the flow sensor at the time of installation, or is indicative of being located in a hydrologically separate zone. However, based on the continuity of the geologic logs and the smoothness of the piezometric surface derived from wells in the FDA, the azimuthal angle for MW-OU1-38-A appears more indicative of an installation error rather than a hydrogeological phenomenon.

As shown in Table 9-4, the ISPFS horizontal velocity estimates after shutdown of EW-OU1-18-A are lower than suggested by the simple model for MW-OU1-36-A

and MW-OU1-37-A. The MW-OU1-36-A flow sensor indicates a reduction in horizontal flow velocity of 42% after pump shutdown, whereas based on the simple model, it is only 7%. Similarly for MW-OU1-36-A, the flow sensor shows a velocity reduction of 41% and the simple model shows a velocity reduction of 27%. The groundwater flow directions for MW-OU1-36-A and MW-OU1-37-A flow sensors are very similar to the simple flow model azimuthal direction. Despite some discrepancies between measurements and the flow model, which may be due to three-dimensional effects and heterogeneity not captured in the simple model, we find the working ISPFSs to be producing plausible data.

Table 9-4. Comparison of horizontal velocities (magnitude and azimuth (Azi.)) from ISPFSs and based on simple flow model.

Well	Flow Sensor Data						Flow Model					
	Pre-Pump Shutdown			Post-Pump Shutdown			Pre-Pump Shutdown			Post-Pump Shutdown		
	Magnitude		Azi.	Magnitude		Azi.	Magnitude		Azi.	Magnitude		Azi.
	ft/day	m/day		ft/day	m/day		ft/day	m/day		ft/day	m/day	
MW-OU1-36-A	0.055	0.017	340°	0.032	0.0097	340°	0.14	0.043	326°	0.13	0.040	317°
MW-OU1-37-A	0.24	0.073	318°	0.14	0.043	315°	0.18	0.055	345°	0.13	0.040	337°
MW-OU1-38-A	0.33	0.10	218°	0.33	0.10	215°	0.12	0.037	326°	0.09	0.027	344°
MW-OU1-39-A	0.09	0.027	318°	*	*	*	0.07	0.021	336°	*	*	*

* No comparison is made because flow sensor experienced power reduction prior to pump shutdown.

10.0 REALTIME CHEMISTRY ANALYSIS

10.1 Chemistry Data Management and File Types

To facilitate rapid retrieval and examination of analytical data, a chronological filing syetem was incorporated into the LabVIEW software that controls the integrated GC/ASAP system . Raw chromatogram data is stored in the native binary format of the plotting package Igor Pro 4 (Wavemetrics, Inc., Lake Oswego, OR.) used to generate all figures in this section. From this file format, other file types can be generated quickly, and even large numbers of data points are rapidly displayed.

Raw GC binary files are saved in an automatically generated, chronological directory structure. Sampling and sample processing take place in programmable sequences, with standards interleaved with samples pumped from wells. After a GC run, the LabVIEW data acquisition application checks the system clock, and then searchs for a directory for the present year in an operator-supplied base directory; if a file for the year is not present (e.g.: C:HardDrive/ASAP files/2001), the subdirectory is created. Similarly, if a subdirectory for the current month and day is not present, those directories are created, so that each day's data files are in a separate subdirectory, identified by date (e.g.: C:HardDrive/ASAP files/2001/10_2001/10_31_2001).

Individual raw data files are also named to facilitate identification for later review. Following a source prefix is a serial number associated with the GC cumulative history, time of day at which the sample was processed, and detector type that generated the signal in the datafile. For example, a sample taken from MW-OU1-04-A at 3:38 PM, and analyzed with the DELCD detector would be named "W04.10483 3.38 PM.DELCD," and a chemical standard would be named "QCC1.10488 6.55 PM.DELCD," for a standard sample from Syringe B (QCC; low-level dilution of commercial standard blend), using ASAP sampling loop 1, sampled at 6:55 PM. This sample naming and directory storage scheme gives complete identification of individual sample sources, generation times and detector types for future analysis.

Broadly speaking, operation of the integrated GC/ASAP system is divided into two parts: sample selection and gas stripping by the ASAP, and analysis and data storage by the GC and a host computer. At this time, peak identification and quantitation is performed off-line with a LabVIEW application separate from the GC control and data acquisition application ("Chromatogram analyzer.VI"); these two modules will be integrated at a later date.

Compounds were identified as described in Section 6.2, by comparison of compound retention times from standard dilutions analyzed with the GC/ASAP system against vendor-published column application examples

(e.g.: Restek, Inc.© Chromatography 2000, p 431), and by running diluted samples of individual compounds, as necessary.

The "Chromatogram Analyzer.VI" LabVIEW application manages the process of compound identification, quantitation, and report generation. The operator starts the analysis process by generating a standard record file, identified by analysis date and a sequential "standard set" number (e.g.: 100401s104.std). This binary file comprises a data structure with all pertinent information on the chromatography system and standard source in use on any given date, including column type and date of installation, expected analyte retention time window, quantity of analyte in the commercially blended standard in use on that date, identified by vendor, catalog number and lot number, and calibration coefficients for each individual analyte's standard curve. Following analysis of any given chromatogram, one of three ascii (text) report types can be generated: a "Run" file (a typical chromatographer's run report, with parameters identifying the sample and the various thresholds and slope factors relevant to peak quantitiation), a "Calibration" file (summarizing analysis of all analytes, giving only retention time and peak areas) usually generated only for standard analyses, or a "Trend" file, that includes sample identity, sample date and time, and calculated sample concentration. The trend files are structured so that plots can be generated from other software packages, such as spreadsheets or other specialized plotting software.

10.2 Analyte identification and quantitation

The "standard record" is the data structure used within the Chromatogram Analyzer.VI application to identify sample compounds by GC retention time, and determine their concentrations. Response curves were first generated from analysis of a range of standard volumes, selected from the sample loops and sample selection valve of the ASAP (Item 11, Figure 6-23). Seven sample loops were used during this study (0.17, 0.31, 0.50, 1.0, 2.29, 4.81 and 9.93 ml, respectively for sample loops one through seven). By using several loop sizes, and two special 100 ml gastight sample syringes, with dilutions that differed tenfold from one another, a range of analyte masses were delivered to the GC for analysis, that bracketed the expected concentrations in well samples.

Method Detection Limits (MDLs) were estimated by analysis of a low-level standards (using loop 2, 0.31 ml from Standard Syringe B; 20 µl Ultra Scientific CLP-150 in 88.0 ml total volume; samples designated with the "QCC2" prefix). The approximately 7 ng of each analyte, had it been present in the 9.93 ml loop used for all well samples, would have represented a sample concentration of about 1 ppb. MDLs were calculated with the EPA approach: seven analyses of a standard sample with concentrations near the expected MDL are run and processed using the routine quantitation method applied to actual samples; the MDL is the

standard deviation of mean for the seven samples. During the testing period of the integrated system, this process was performed by selecting the QCC2 runs from seven sequential sets of standards interleaved with well samples, so that the runs were actually performed over about two days. Nonetheless, MDLs for all halogenated compounds present in the standard blends were below 1 ppb, as shown in Table 10-1. This table also summnarizes analyte retention times, quantities in the concentrated standard blend used, and detection patterns for wells at the OU 1 FDA, sampled both with manual means in the two quarters prior to installation of the instrument monitoring facility, and with the GC/ASAP system.

10.3 Chemical trends in ASAP operation and OU 1 wells

The automated nature of the GC/ASAP system supports a variety of techniques to continually validate performance. In addition to regular estimation of MDLs, the stability of standard analysis can be used to detect detector drift or other problems. In a "well-tuned" state, the integrated system is capable of very stable recover of standards, as shown in Figure 10-1.

In the final testing of the integrated system, standards and samples were processed continuously, starting in early October, 2001. Typical chromatograms from each of the ten wells sampled, and trends for analytes detected above the MDLs are shown in Figures 10-2 through 10-11.

Table 10-1. Analytes of interest at Fort Ord, OU 1. Shown are compounds present in commercially prepared standards used with the On-Line analytical system (Ultra Scientific, Inc., CLP-150, Lot P0929), their weights in the concentrated standard blend, detectability by the On-Line GC detector, GC retention times (RTs), method detection limits (MDLs) measured with the On-Line system, wells with compounds detected by manual sampling in the two quarters prior to automated sampling, and wells with analytes detected with the On-Line system in October, 2001. Compounds in boldface are identified as "Chemicals of Concern" in either (or both) the OU 1 and OU 2 Records of Decision.

Cmpd	Abbrev.	Weight/ml (CLP-150 std)	Analytes detected by SRI DELCD	RT[1](min.)	Oct '01 On-line MDL (µg/L)	OU 1 wells with analytes detected in Oct '00 to Mar '01 sampling[4]	OU 1 wells with analytes detected with On-line system at OU1, 10/01
chloromethane	CH3Cl	100.4	+[2]	3.301	-		
vinyl chloride	VC	100.4	+	3.460	0.49		
bromomethane	CH3Br	100.4	+	4.239	0.43		
chloroethane	C2H5Cl	100.4	+[3]		-		
acetone	ACE	100.4					
1,1-dichloroethene	1,1-DCE	100.4	+	5.775	0.47	4	37, 39
carbon disulfide	CS2	100.4					
methylene chloride	CH2Cl2	100.4	+	6.831	0.84		
trans-1,2-dichloroethene	t-1,2-DCE	100.4	+	7.440	0.65		7, 20[5], 39, 40
1,1-dichloroethane	1,1-DCA	100.4	+	8.366	0.76	4, 39	4, 5, 7, 19[5], 20, 36, 37, 38[5], 39, 40[5]
cis-1,2-dichloroethene	c-1,2-DCE	100.4	+	9.624	0.79	4, 20, 39	4[5], 5[5], 7, 19, 20[5], 36[5], 37, 38[5], 39, 40
chloroform	CHCl3	100.4	+	9.948	0.82	4, 20, 39	4[5], 5[5], 7, 19[5], 20[5], 36[5], 37, 38[5], 39, 40[5]
2-butanone	2-BUT/MEK	100.4					
1,1,1-trichloroethane	1,1,1-TCA	100.5	+	10.748	0.50	4, 5, 19, 20, 37, 39	4, 5, 7, 19, 20, 36, 37, 38, 39, 40
carbon tetrachloride	CCl4	100.4	+	11.235	0.45		

benzene	BEN	100.3					
1,2-dichloroethane	1,2-DCA	100.4	+	11.601	0.74		7, 20, 39[5], 40
trichloroethene	TCE	100.4	+	12.846	0.68	4, 5, 7, 19, 20, 36, 37,38, 39, 40	4, 5, 7, 19, 20, 36, 37, 38, 39, 40
1,2-dichloropropane	1,2-DCPA	100.5	+	13.215	0.84		
bromodichloromethane	CHBrCl2	100.5	+	13.683	0.84		
cis-1,3-dichloropropene	c-1,3-DCPE	100.5	+	14.789	0.81		4[5], 5[5], 7, 19[5], 20[5], 39[5], 40[5]
4-methyl-2-pentanone	MIBK	100.2					
toluene	TOL	100.3					
trans-1,3-dichloropropene	t-1,3-DCPE	100.5	+	15.818	0.82		4[5], 5[5], 7, 19[5], 20[5], 37[5], 39[5], 40[5]
1,1,2-trichloroethane	1,1,2-TCA	100.4	+	16.128	0.78		7, 20, 39[5], 40
tetrachloroethene	PCE	100.3	+	16.761	0.53	39	4, 5[5], 7, 19, 20, 36, 37, 38, 39, 40
2-hexanone	2-HEX	100.3					
dibromochloromethane	CHBr2Cl	100.5	+	17.181	0.86		
chlorobenzene	BENCl	100.4	+	18.491	0.82		7[5], 20[5], 39[5], 40[5]
ethylbenzene	Eth-BEN	100.3					
m-xylene	m-XYL	100.3					
p-xylene	p-XYL	100.2					
styrene	STY	100.4					
o-xylene	o-XYL	100.4					
bromoform	CHBr3	100.5	+	20.450	0.75		
1,1,2,2-tetrachloroethane	1,1,2,2-TCA	100.4	+	20.799	0.73		

[1]RT = retention time for Restek 505.2 column (60m x 0.32 mm I.D., 1.5 μ film).
[2]Chloromethane was detectable in standards, but with a distorted baseline that prevented reliable quantitation; it was not observed in any well samples.
[3]May not be separated from bromomethane; one peak at 4.239 min. reported as bromomethane for this report. No peaks at this retention time observed in any well samples.
[4]MW-OU1-36-A was not manually sampled in either the Oct-Dec '00 or Jan-Mar '01 monitoring periods.
[5]Observed, but not detected above the On-Line MDL.

11.0 FLOW AND TRANSPORT MODELING

11.1 Introduction

We developed a 3D simulation grid based on the hydrostratigraphic model (Section 7) and carried out flow and transport modeling aimed at furthering our understanding of groundwater flow and transport at OU 1. Because the focus in the current project is on understanding flow in the saturated A-aquifer in support of testing and application of the network of new sensors, we have concentrated our modeling efforts on the saturated zone. Nevertheless, the simulations are all unsaturated-saturated, i.e., multiphase, with flow and transport processes occurring in both the unsaturated and saturated zones. In this section, we summarize our work on 3D numerical simulation of flow and transport at OU 1.

11.2 Grid Generation

The domain of simulation covers an area 0.33 mi^2 (0.86 km^2) and approximately 150 ft (46 m) deep surrounding the FDA as shown in Figure 11-1. With this region defining the lateral extent of the domain, and the locations of numerous wells specified as gridblock centers, we used Wingridder (Pan et al., 2001) to generate a 2D (X, Y) mapview discretization consisting of 1056 gridblocks as shown in Figure 11-2. The region shaped like a parallelogram oriented northwest-southeast apparent in the discretization was designed to facilitate subgrid calculations that focus on the FDA. Elevations and thicknesses of the various layers and topography from the hydrostratigraphic model (e.g., Figure 7-2) are input into Wingridder to generate the 3D model consisting of irregular layer-conforming gridblocks in the Z-direction extending upward from mean sea level along the columns shown in Figure 11-2. The result is a 3D numerical grid for TOUGH2 consisting of 31,888 gridblocks with 105,154 connections between gridblocks. The 3D grid is shown in an oblique view in Figure 11-3 to highlight the topography of the top surface and irregular clay layers near the bottom of the grid. Properties of the sediments are assigned based on generalized sand (Moridis et al., 1999) and clay (Leij et al., 1996) properties as given in Tables 11-1 and 11-2. Although unsaturated flow properties are given in the Table 11-1 (e.g., van Genuchten, 1980), we emphasize that the focus of this study is on saturated zone flow.

Table 11-1. Capillary pressure parameters used in simulations (CP(n) are the TOUGH2 input variable names).

Unit	α (1/m)	α *(1/Pa) (CP(3))*	*n*	λ *(CP(1))*	S_{lr} *(CP(2))*	S_{ls} *(CP(5))*	$P_{cap\ max}$ (Pa) *(CP(4))*
Sand	8.2	8.4×10^{-4}	2.46	0.59	0.10	1.	-1.0×10^{5}
Clay	0.80	8.2×10^{-5}	1.09	0.083	0.34	1.	-5.0×10^{6}

α is van Genuchten's α; λ is van Genuchten's $\lambda = 1\text{-}1/n$; S_{lr} is residual-liquid saturation; S_{ls} is satiated saturation; $P_{cap\ max}$ is maximum capillary pressure.

Table 11-2. Porosity and permeability used in simulations.

Unit	porosity	permeability (m^2)
Sand	0.30	2.0×10^{-12}
Clay	0.20	1.0×10^{-15}

11.3 Simulated Water Table Elevation

A steady-state flow field has been simulated using the EOS9 module of TOUGH2 and based on the 2000 water table (piezometric surface). The procedure used involves setting the boundary gridblock water table elevations at the level specified by the contoured data surface (Figure 8-5) by setting boundary gridblocks (i.e., those on the vertical edges of the model domain at the elevation of the water table) to be inactive with constant liquid saturation of 0.5 and zero capillary pressure. This causes all gridblocks below the inactive gridblock to fill up with water, and those above to drain to a gravity-capillary equilibrium. The discretization in the vertical direction means that the water table elevations can only be set to approximately ±1 m or so, a level of certainty comparable to the certainty of the contoured data. Once vertical equilibrium is achieved in each column, the boundary columns are set inactive and used as the boundary conditions for the entire 3D flow system.

The boundary conditions of time-invariant piezometric head specified along each of the north, south, east, and west boundaries create a flow system with generally northwest flowing groundwater. The conceptual model includes a uniform percolation flux through the unsaturated zone that recharges the A-aquifer. A precipitation recharge rate of 1.4 in/yr (3.5 cm/yr) was arrived at by trial and error simulation until the water table elevations grossly matched those in Figure 8-5. This recharge is 1/12 (8.2%) of the average annual precipitation of 17 in/yr (43 cm/yr). This result disagrees with the estimate of Section 8.11, where it was estimated that 27% of precipitation recharges the aquifer. This disagreement is not

unexpected, given that the water table elevation is a result of complex interactions between recharge and permeability, a property assumed spatially invariant in the modeled sand and clay layers. Furthermore, any attempt to fit a recharge rate conditioned on water table elevations should be carried out in concert with permeability fitting, a process that would be poorly constrained by available data, and therefore was not undertaken here. The conceptual model also includes the GTS consisting of extraction from EW-OU1-18-A and EW-OU1-17-A along with recharge of treated water in the southern part of the FDA by sprinkler. Pumping rates for the two wells were set to rates current in November 1999. The recharge by sprinkler that roughly matched Figure 8-5 was equal to one-third the rate of water treated. For both the precipitation and sprinkler recharge rate, the water table was matched by hand rather than by inversion methods, an approach considered appropriate given the sparseness of water level data. These parameters used in the simulation are summarized in Table 11-3.

Table 11-3. Recharge and pump parameters for steady-state flow simulation.

Unit	Pumping rate from EW-OU1-17-A	Pumping rate from EW-OU1-18-A	Precipitation Recharge Rate	Sprinkler recharge rate
English	9.0 gpm	8.5 gpm	1.4 in/yr	5.8 gpm
metric	5.7×10^{-4} m^3/s	5.4×10^{-4} m^3/s	3.6 cm/yr	3.7×10^{-4} m^3/s

The simulated steady-state piezometric head and flow field at an elevation of Z = 14 m is shown in Figure 11-4. Comparison against Figure 8-5 shows that the gross features of OU 1 hydrology are captured. In particular, the drawdowns around EW-OU1-17-A and EW-OU1-18-A are well represented. The groundwater mound at the sprinkler recharge area is visible in the figure as the pointed, angular contour lines near X = 2200 m, Y = 3050 m. This mound causes the outward bowing of the nearby flowlines, which are shown in black. The small markers on the flow lines represent the distance a particle would travel in 10 years. No flowlines significantly different from the generalized water table gradient were observed at any elevation. Although the gradients on the west side of the Airfield Clay and around EW-OU1-17-A are smaller in the simulation than in Figure 8-5, Darcy velocities in sands below the FDA are on the order of 0.2 ft/day (0.06 m/day), in good agreement with flow sensor data (cf. Table 9-4). This result confirms the prior finding that tracer tests in OU 1 will require long time periods over which to observe tracer transport for well spacings on the order of 100 ft (30 m).

Figure 11-5 shows the same simulation result in three slices through the 3D domain, where head (ft) is contoured and the vectors represent pore

velocities. Figure 11-6 shows the corresponding liquid saturation and pore velocities. The X-plane slice in these figures was chosen to intersect the sprinkler recharge area and shows clearly the resulting percolation flux and larger liquid saturation associated with percolation of treated water through the unsaturated zone.

11.4 Capture Zone with Sprinkler Off

In this section, we present a simulation result corresponding to a change in the manner of disposal of treated groundwater. This simulation is motivated by the hypothesis that recharging treated water upgradient from the GTS may tend to cause short-circuiting of the flow field, and give rise to a smaller capture zone than if treated water were discharged in some other manner. Motivation for this potential new approach comes also from the observations of the ecologists managing the nature preserve that the sprinkler encourages non-native vegetation. Figure 11-7 shows a steady-state flow field for conditions identical to those of Figure 11-4 except that the sprinkler recharge has been turned off. As can be seen by comparison of Figures 11-7 and 11-4, the capture zone upgradient of the GTS is considerably wider on the east side when sprinkler recharge is turned off. This result confirms the hypothesis that recharging treated groundwater results in a short-circuit of the GTS and is non-optimal from the point of view of maximizing the size of the capture zone. Additional ecological reasons may also motivate rethinking of the method of disposal of treated groundwater.

11.5 Flow with EW-OU1-18-A Turned Off

During the course of our investigations at OU 1, EW-OU1-18-A was turned off, an event that we exploited as a perturbation for ISPFS response testing (Section 9). In Figure 11-8, we present the simulated steady-state flow field for OU 1 with EW-OU1-18-A turned off. As shown, the simulation results in a smaller capture zone and decreased mounding at the recharge area for this case where only EW-OU1-17-A extracts water at 9.5 gpm (5.7×10^{-4} m^3/s) and one-third of this water applied by the sprinkler recharges the aquifer. Note that Figure 11-8 is the steady-state flow field, a condition the actual flow field at OU 1 may not yet have attained.

11.6 Simulated TCE Plume Evolution

The shape of the current TCE plume has been a source of great interest at OU 1. As currently understood, the TCE plume appears to move northward near the source at the FDA and then turn northwestward, despite water table gradients that generally point northwestward at the present time. Possible causes of the TCE plume configuration include permeability anisotropy (e.g., Quiñones-Aponte, 1989) subsurface high-permeability channels (HLA, 1998a), and additional source areas of TCE

contamination. In this section, we extend our simulation results of flow to consider the transport of TCE and possible evolution of the OU 1 plume from the time of its origins until the present day. We use the TOUGH2 module T2VOC for these simulations.

Recall the perimeter-well water table discussed in Section 8.8 represents a possible pre-pumping water table. We developed a steady-state simulation for this perimeter-well water table to be used with T2VOC for TCE transport simulation. The simulated perimeter-well water table is shown in Figure 11-9, and can be compared against the 2000 water table as shown in Figure 8-5. With this perimeter-well water table and flow field as the initial condition, we introduced a source of TCE of strength 10 kg/yr for 20 yrs (say from 1968 to 1988) below the former burn pit in the FDA. We present in Figure 11-10 the resulting TCE plume after 20 yrs. The contours represent the TCE concentration as mass fraction in the liquid (X_{liq}^{TCE}), where $X_{liq}^{TCE} \times 10^9$ [=] ppb. A small amount of retardation is included in this calculation through the inclusion of a small fraction organic carbon (FOC) equal to 0.0001. Note the extensive spreading of the plume due to both advection and numerical dispersion. Additional spreading is due to gas-phase diffusion occurring in the deep unsaturated zone above the groundwater plume, and subsequent partitioning of gas-phase TCE back into the water in the capillary fringe (e.g., Falta et al., 1989).

Starting from the simulated 1988 conditions of Figure 11-10, we change the flow field to correspond to the current GTS flow field (see Figure 11-4) and combine this flow field with the simulated 1988 TCE concentration field as an initial condition. In Figure 11-11 and 11-12, we present the TCE concentration fields and flow lines at t = 5 and 12 yrs, representing the years 1993 and 2000, respectively. Note that the GTS has reduced TCE concentrations at EW-OU1-17-A to between 10 and 100 ppb, while concentrations at EW-OU1-18-A are just over 1 ppb, in rough agreement with quarterly data (Section 8.13). Although the effects of dispersion appear much larger in the simulation than in plume contour maps (e.g., Figure 8-34), one can discern the slight bend in trajectory of the plume from northward prior to operation of the GTS to northwestward after the GTS was turned on. This is a fundamental feature of the current TCE plume. This simulation shows one possible scenario for the current plume configuration. Namely, the pre-pump head gradients caused the plume to migrate northward, while the current gradient causes it to migrate northwestward. By this scenario, no additional sources of TCE are required, nor must we appeal to anisotropy or buried flow channels to explain the plume shape. Essentially, the current plume configuration is a natural outcome of a single source at the FDA and a time-varying A-aquifer water table.

12.0 CONCLUSIONS

12.1 Specific Hydrologic Questions

The four specific hydrologic questions and our findings are presented below.

(1) Was the Fire Drill Area (FDA) the source of the northwestern plume discovered in 1997?

Finding: It appears from analysis of hydrographs and contaminant concentration trends that no additional source areas of TCE beyond the immediate area of the FDA have contributed to the northwestern plume (Sections 8.12 and 8.13). From numerical simulation analyses (Section 11.6), it appears that a pre-pumping water table gradient that may have been directed more northerly than the present water table gradient caused advection of the plume downgradient of the GTS prior to its startup in 1988. This result agrees with the conclusions of Harding ESE (2001).

(2) How do clay bodies and flow channels affect the pump-and-treat process?

Finding: The clay bodies below the area around the FDA form low-permeability barriers to flow and transport. These layers can isolate zones in the A-aquifer from the effects of the GTS (Section 8.9). The fact that numerical simulations of flow and transport at OU 1 do not show isolated zones points to the possible existence of additional clay bodies not formally defined in the hydrostratigraphic model used in the flow simulations (Section 11.3). Data analysis in this project did not suggest the existence of flow channels, except insofar as sandy regions without siginficant clay bodies form high effective permeability zones. Accordingly, the hydrostratigraphic model does not define flow channels (Section 7.4).

(3) Why are TCE concentrations increasing at certain wells?

Finding: Detailed analysis of quarterly data suggests that downward percolation of precipitation and treated recharge water may be flowing through contaminated regions in the unsaturated zone below the FDA and transporting contaminants down to the water table (Section 8.13). The data suggest that remnant unsaturated zone sources may exist within a couple hundred feet (<70 m) west or northeast of the FDA fence, but the exact locations are not known.

(4) What is the impact on the GTS of infiltrating treated water within the capture zone?

Finding: Infiltrating treated water within the capture zone tends to short-circuit the GTS and decrease the width of the capture zone (Section 11.4). In addition, infiltrating treated water may be mobilizing remnant unsaturated zone contamination and causing concentration increases at wells within the capture zone (Section 8.13).

12.2 General Conclusions

Hydrostratigraphic model development

A three-dimensional hydrostratigraphic model capturing multiple clay and sand layers in the shallow subsurface has been developed based on lithologic information from 70 wells located throughout the OU 1 area. This model has been used as the basis for generating a numerical grid for simulating and evaluating the flow and contaminant transport behavior within the A-aquifer and the FO-SVA at OU 1.

Installation and testing of chemical analysis system

A micropurged sample acquisition and sample analysis sytem has been installed that provides integrated, on-line instrumention on the scale of an entire remediation site. The analytical equipment successfully supports relatively unattended operation for extended periods, and has demonstrated stability, sensitivity and precision comparable to formal analytical laboratory instruments over at least the time scale of weeks. Moreover, since samples are transported through a highly inert, all-metal sampling system, they apparently arrive at the analytical hardware in a relatively undisturbed state, as analytes not detected with manual sampling and formal laboratory analysis were frequently detected, and other compounds, although previously found at the site, were detected in wells where they had not been previously observed. Although during testing data acquisition and subsequent quantitation and reporting were separate processes, these can be integrated in the future to provide integration, and instantaneous updates of contaminant distributions.

Analysis of quarterly data

The average precipitation over the last 10 years at OU 1 is 17.1 in/yr. In 1998, OU 1 had more than twice the average annual precipitation, and this precipitation is causing some wells to continue to rise at present. The large 1998 rainfall causes the cones of depression around the extraction wells to decrease, leading to smaller capture zones.

The water table shows a generalized northwest gradient, with largest hydraulic gradients near the edge of the Airfield Clay adjacent to the extraction well EW-OU1-17-A. Combining the observed gradient in the FDA with an estimate of hydraulic conductivity suggests a conservative tracer would move at 0.21 ft/day (0.064 m/day), leading to 450-day transport for a conservative tracer over 100 ft (30 m).

Piezometric head beneath the Airfield Clay is approximately the same as the head at EW-OU1-17-A, implying that flow could move under the Airfield Clay as well as toward the extraction well. Piezometric heads in sands confined by clay layers in the FO-SVA screened in well MW-OU1-11-SVA fluctuate seasonally more

than unconfined A-aquifer sands, indicating the possibility of lateral recharge, for example from the Salinas River. A large downward gradient exists between the confined sands within the FO-SVA and the 180-foot aquifer. The gradient in the 180-foot aquifer is toward the southeast, possibly controlled by agricultural pumping.

- The hypothetical pre-extraction water table (perimeter-well water table) gradient points north from the FDA in contrast to the 2000 water table gradient which points northwestward.

Examination of water level changes in EW-OU1-18-A shows that MW-OU1-07-A and MW-OU1-12-A are not hydraulically connected, a fact also observed during pump testing. Similarly, EW-OU1-17-A appears not to communicate above and below the Airfield Clay, implying that the Airfield Clay is a barrier to effective pump and treat. As water levels increase in the extraction wells, they decline in the recharge area on a 45–60 day time scale. The rapid response of the water table below the recharge area suggests that there are no significant low-permeability layers in the unsaturated zone.

Comparing rainfall amounts to water level increases suggests that approximately 27% of precipitation ends up as recharge at the A-aquifer. The infiltration pulse signal travels 60 ft (18 m) through the unsaturated zone in less than one month. For thicker unsaturated zones, the pulse travels at 20 ft/mo (6.1 m/mo).

Groundwater at OU 1 is contaminated with VOCs, primarily TCE. Recent increases in TCE concentration at wells to the west of the FDA are likely due to treated recharge encountering residual contamination in the unsaturated zone and transporting it to the water table. TCE concentration increases above the Airfield Clay may be indicative of an additional source approximately 200 ft (61 m) northeast of the FDA. However, the northwest plume is generally down-gradient from the FDA, suggesting the general area of the FDA is the source area for the northwest plume. Examination of concentrations of TCE degradation products suggests that reductive dechlorination is not occurring at OU 1.

ISPFS testing

The qualitative changes observed in the piezometric surface indicate that the groundwater velocities in the FDA are reduced after shutdown of EW-OU1-18-A. These reductions are clearly visible in the ISPFS data with changes corresponding to the exact time when pumping stopped. The magnitude of velocity reduction observed in the ISPFS is greater than suggested by the simple flow model. Because of uncertainty in formation properties it is reasonable to expect discrepancies between the ISPFS data and the simple model. Similar to the large apparent downward velocities observed, the calculated horizontal velocities may be subject to thermal heterogeneity of the formation. Nevertheless, we find the ISPFSs to be a sensitive instrument capable of realtime groundwater velocity measurement.

Simulations of flow and transport

Numerical simulation analyses show that the effects of the clay layers as defined in the hydrostratigraphic model do not lead to flow directions significantly different from the generalized water table gradient. Simulations also show that infiltrating treated groundwater upgradient from the GTS causes a groundwater mound that decreases the width of the capture zone. TCE transport simulations show that a time-varying water table with northward gradient prior to startup of the GTS and northwestward gradient after startup of the GTS can produce a bent plume as observed in the chemistry data.

13.0 RECOMMENDATIONS

Applications of ICFMS

Test and evaluate the long-term application of the new sensor technologies to the operational scale remediation activities of the GTS. Operation of these new technologies on a sustained basis will help to assess the effectiveness and cost efficiencies of the new sensors.

Take advantage of the rapid response of the ICFMS for chemistry, velocity, and pressure to constrain better the location of potential unsaturated zone remnant VOC contamination sources during infiltration events.

Operate the automated sampling system through the winter and spring months to capture data from natural recharge events that may constrain unsaturated zone flow and transport processes

Correlate short term ISPFS velocity variations with short term oscillations in analyte concentrations. Research in this area may reveal new details about groundwater plume dynamics.

Monitoring and Site Remediation

Continue quarterly monitoring of contaminants and water levels, as this data set has been invaluable in our research and for understanding key features of the A-aquifer at OU 1.

Perform soil gas monitoring with multilevel vadose zone monitoring wells in the unsaturated zone at depth to monitor soil gas concentration changes in response to natural and artificial recharge changes to help locate potential remnant contamination.

Consider disposing of treated water in a different way than recharging in the capture zone. Possible options include misting the water so it evaporates into the air, or discharging it downgradient from the GTS.

Consider alternate locations of disposing of treated water. Additional deployments of ISPFSs could be done to monitor flow directions quickly and accurately such that targeted vadose zone regions could be intentially flushed with subsequent guidance of the resulting recharge toward the extraction wells through selected recharge locations.

Increase the pumping rate from EW-OU1-17-A. This could have several benefits for remediation investigations at OU 1: (1) It would increase the size of the capture zone which seems to have shrunk after 1998; (2) It could serve as a pump test, the response to which could be used to understand the well's effectiveness at controlling downgradient migration of contaminated water from above the Airfield Clay; and (3) the increase

in recharge rate resulting from increased pumping at EW-OU1-17-A could be coupled with results from the automated sample analysis system to test the hypothesis that TCE residing in the vadose zone west of the FDA is mobilized into the water table in this area by large recharge events.

Use alternate locations for treated water discharge as a simple substitute for pump tests as a flow system perturbation in future hydrologic testing at OU 1.

Modeling

Revise and update the hydrostratigraphic model as additional lithostratigraphic data become available from new wells for future flow and transport modeling studies.

Revise interpreted areas within the hydrostratigraphic model domain (where little or no lithologic data exist) as additional indirect indicators of subsurface lithology become available, such as water level responses to pumping, spatial variability in water chemistry, and geophysical surveys.

Carry out non-isothermal simulations of flow around a simulated ISPFS to evaluate apparent vertical flow and develop confidence in the estimated horizontal velocity.

Carry out additional TCE transport simulations to investigate the large dispersion observed in the model results relative to the contoured TCE plume. Consider using particle tracking methods instead of multicomponent transport to decrease numerical dispersion.

References

Atwater, B.F., C.W. Hedel, and E.J. Helley, 1977. Late Quaternary depositional history, Holocene sea-level changes, and vertical crustal movement, southern San Francisco Bay, California, U.S. *Geological Survey Professional Paper 1014*, U.S. Government Printing Office, Washington D.C.. 15 pp.

Ballard, S., 1995. Ground water flow velocity in the bank of the Columbia River, Hanford, Washington, Sandia National Laboratory Report *SAND95-2187*, Sandia National Laboratory.

Ballard, S., 1996. The in situ permeable flow sensor: A ground-water flow velocity meter, *Groundwater 34*(2), 231-240.

Ballard, S., G.T. Barker, and R.L. Nichols, 1996. A test of the in situ permeable flow sensor at Savannah River, SC, *Groundwater 34*(3), 389-396.

Barcelona, M.J., H.A. Wehrmann, and M.D. Varljen, 1994. Reproducible well-purging procedures and VOC stabilization criteria for ground-water sampling. *Ground Water* 32(1), 12-22.

Birkeland, P.W., 1972. Late quaternary eustatic sea-level changes along the Malibu coast, Los Angeles County, California, *Journal of Geology*, *80*, 432–448.

Calder, T., 1998. Farmnote: Efficiency of sprinkler irrigation systems, http://www.agric.wa.gov.au/agency/Pubns/farmnote/1992/f04892.htm, Agriculture Western Australia.

Daley, P.F. 1992. Automated monitoring of a soil remediation system. *Scientific Computing and Automation*, 8(6), 23-28.

Falta, R.W., and I. Javandel, K. Pruess, and P.A. Witherspoon, 1989. Density-driven flow of gas in the unsaturated zone due to the evaporation of volatile organic compounds, *Water Resour. Res.*, *25*(10), 2159–2169.

Falta, R. W., K. Pruess, I. Javandel, and P. A.Witherspoon. 1992a. Numerical modeling of steam injection for the removal of nonaqueous phase liquids from the subsurface 1. Numerical formulation., *Water Resour. Res.*, *28*, 433–449.

Falta, R. W., K. Pruess, I. Javandel, and P. A. Witherspoon. 1992b. Numerical modeling of steam injection for the removal of nonaqueous phase liquids from the subsurface 2. Code validation and application. *Water Resour. Res.*, *28*, 451–465.

Falta, R. W., K. Pruess, S. Finsterle, and A. Battistelli. 1995. T2VOC User's Guide, Lawrence Berkeley Laboratory Report, LBL-36400, Berkeley, California (March 1995).

Fisher, A., D. Underwood, J. Erskine, J. Duey. S. Lewis, E. Silver, J. Gill, and N. Narisimhan, 1998. Geological, geophysical, and hydrogeological characterization of shallow aquifers and confining layers near the OU2 Landfill, former Fort Ord, CA. Final Report of the Fort Ord Landfill Demonstration Project, U.C. Santa Cruz.

Fries, M.R., G.D. Hopkins, P.L. McCarty, L.J. Forney, and J.M. Tiedje, 1997. Microbial succession during a field evaluation of phenol and toluene as the primary substrates for trichloroethene cometabolism. *App. Environ. Microbiol. 63*(4), 1515-1522.

Harden, D.R., 1998. *California Geology*, Prentice Hall, New Jersey, 479 pp.

Harding ESE, 2001, Revision B, Phase V well installation report Operable Unit 1, former Fort Ord, California, Harding ESE, Novato, CA, June 8.

Harding Lawson Associates (HLA), 1993. Draft Basewide Hydrogeologic characterization Fort Ord, California Volume I – Text and Plates, Harding Lawson and Associates, Novato, CA, June 7.

Harding Lawson Associates (HLA), 1994. Draft Final OU 1 Remediation Confirmation Study, Fritzsche Army Airfield Fire Drill Area, Fort Ord, California, Harding Lawson and Associates, Novato, CA, May 3.

Harding Lawson Associates (HLA), 1998a. Volume I – Site Investigation Operable Unit 1 Plume Delineation Report, Former Fort Ord, California, and Volume II – Draft Work Plan for Preliminary Remedial Evaluation Operable Unit 1 Plume Delineation Former Fort Ord, California, Harding Lawson and Associates, Novato, CA, April 29.

Harding Lawson Associates (HLA), 1998b. Operable Unit 1 Groundwater Treatment System Report of Semiannual Monitoring (October 1997 through March 1998), Fort Ord, California, Harding Lawson and Associates, Novato, CA, July 14.

Hopkins, G.D. and P.L. McCarty, 1995. Field evaluation of in situ aerobic cometabolism of trichloroethylene and three dichloroethylene isomers using phenol and toluene as the primary substrates. *Environ. Sci. Technol., 29*(6), 1628-1637.

Hopkins, G.D., J. Munakata, L. Semprini, and P.L. McCarty, 1993. Trichloroethylene concentration effects on pilot field-scale in situ groundwater bioremediation by phenol-oxidizing microorganisms. *Env. Sci. Technol., 27*(12), 2542-2547.

Hopkins, G.D., L. Semprini, and P.L. McCarty, 1993. Microcosm and in situ field studies of enhanced biotransformation of trichloroethylene by phenol-utilizing microorganisms. *App. Environ. Microbiol.*, 59(7), 2277-2285.

Kearl, P.M. and C.M. Case, 1992. Direct field measurement of groundwater velocities. *Interdisciplinary Approaches in Hydrology and Hydrogeology,* American Institute of Hydrology. pp 91-102.

Kearl, P.M., N.E. Korte, and T.A. Cronk, 1992. Suggested modifications to ground water sampling procedures based on observations from the colloidal borescope. *Ground Water Monitoring Review.* 12(2): 155-161.

Kearl, P.M., N.E. Korte, M. Stites and J. Baker, 1994. Field comparison of micropurging vs. traditional ground water sampling. *Ground Water Monitoring and Remediation., 14*(4): 183-190.

Kerfoot, W.B. and V.A. Massard, 1985. monitoring well screen influence on direct flowmeter measurements. *Ground Water Monitoring Review.*, 5(4): 74-77.

Leij, F.J., W.J. Alves, M.Th. vanGenuchten, and J.R. Williams, 1996. *The UNSODA Unsaturated Soil Hydraulic Database, User's Manual Version 1.0*, U.S. E.P.A., EPA/600/R-96/095.

MacKay, D.M., R.D. Wilson, M.J. Brown, W.P. Ball, G. Xia, and D.P. Durfee, 2000. A controlled field evaluation of continuous vs. pulsed pump-and-treat remediation of a VOC-contaminated aquifer: site characterization , experimental setup, and overview of results. *J.Contaminant Hydrology.* 41: 81-131.

McCarty, P.L., M.N. Golz, G.D. Hopkins, M.E. Dolan, J.P. Allan, B.T. Kawakami, and T.J. Corrothers, 1998. Full-scale evaluation of in situ cometabolic degradation of trichloroethylene in groundwater through toluene injection. *Environ. Sci. Technol., 32*: 88-100.

Moridis, G.J., S. Finsterle, and J. Heiser, 1999. Evaluation of alternative designs for an injectable subsurface barrier at the Brookhaven National Laboratory site, Long Island, NY, *Water Resour. Res., 35*(10), 2937–2953.

Muller, R. A. and T. M. Oberlander, 1984. *Physical Geography Today*, Third Edition. Random House, New York.

NOAA, 1999, National Oceanic and Atmospheric Administration, National Climate Data Center (NCDC) Daily Station, http://ingrid.ldgo.columbia.edu/SOURCES/.NOAA/.NCDC/.DAILY/.STATION.cuf/IWMO/724836/VALUES/.mean.

Pan, L., J. Hinds, C. Haukwa, Y.-S. Wu, and G. Bodvarsson, 2001. WinGridder, an interactive grid generator for TOUGH2, v. 1.0, Lawrence Berkeley National Laboratory Report, *LBNL-42957*, Lawrence Berkeley National Laboratory, July.

Powell, R.M.; and R.W. Puls, 1993. Passive sampling of groundwater monitoring wells without purging-multilevel well chemistry and tracer disappearance, *J. Contam. Hydrol., 12*(N1-2), 51–77.

Pruess, K., 1987. TOUGH user's guide, Lawrence Berkeley Laboratory, Report LBL-20700, Berkeley, CA, and Nuclear Regulatory Commission Report NUREG/CR-4645, Washington, D.C..

Pruess, K., 1991. TOUGH2, a general-purpose numerical simulator for multiphase fluid and heat flow, Lawrence Berkeley Laboratory, Report LBL-29400, Berkeley, CA, May.

Pruess, K., C. Oldenburg, G. Moridis, 1999. TOUGH2 User's Guide, Version 2.0, Lawrence Berkeley National Laboratory Report, LBNL-43134, Berkeley, California.

Puls, R.W., D.A. Clark, B. Bledsoe, R.M. Powell, and C.J. Paul, 1992. Metals in ground water: Sampling artifacts andreproducibility. *Hazardous Waste and Hazardous Materials.* 9(2): 149-162.

Quiñones-Aponte, V., 1989, Horizontal anisotropy of the principal ground-water flow zone in the Salinas alluvial fan, Puerto Rico, *Ground Water*, *27*(4), 491–500.

Rivett, M.O., S. Feenstra, and J.A. Cherry, 2001. A controlled field experiment on groundwater contamination by a multicomponent DNAPL: Creation of the emplaced-source and overview of dissolved plume development, *J. Contaminant Hydrology*, 49: 111-149.

Roberts, P.V., G.D. Hopkins, D.M. Mackay, and L. Semprini, 1990. A field evaluation of in situ biodegradation of chlorinated ethenes: Part 1, Methodology and field site characterization, *Ground Water*, *28*(4), 591-604.

Robin, M.J.L. and R.W. Gillham, 1987. Field evaluation of well purging procedures. *Ground Water Monitoring Review.* 7(4): 85-93.

Semprini, L., G.D. Hopkins, P.L. McCarty, and P.V. Roberts, 1992. In situ transformation of carbon tetrachloride and other halogenated compounds resulting from biostimulation under anoxic conditions, *Environ. Sci. Technol.*, *26*(12), 2454-2461.

Semprini, L., G.D. Hopkins, P.V. Roberts, D. Grbic-Galic, and P. McCarty, 1991. A field evaluation of in situ biodegradation of chlorinated ethenes: Part 3, Studies of competitive inhibition, *Ground Water*, *29*(2), 239-250.

Semprini, L., P.V. Roberts, G.D. Hopkins, and P.L. McCarty, 1990. A field evaluation of in situ biodegradation of chlorinated ethenes: Part 2, Results of biostimulation and biotransformation experiments, *Ground Water*, *28*(5), 715-727.

Smedes, H.W., N. Spycher, and R.L. Allen, 1993. Case history of one of the few successful superfund remediation sites: A site at Salinas, California, USA, *Engineering Geology*, *34*, 189–203.

Tinsley, J.C. III, 1975. Quaternary geology of northern Salinas Valley, Monterey County, California, Stanford University, Ph.D. thesis.

U.S. Army Corps of Engineers (USACE), 1997. Final Report, Groundwater Investigation at Fritzsche Army Airfield, Fort Ord, California, April.

van Genuchten, M. Th., 1980. A closed-form equation for predicting the hydraulic conductivity of unsaturated soils, *Soil Sci. Soc. Am. J.*, *44*, 892–898.

Ernest Orlando Lawrence Berkeley National Laboratory
One Cyclotron Road | Berkeley, California 94720

Prepared for the U.S. Department of Energy under Contract No. DE-AC03-76SF00098